iScience

CellPress

Article

Transcriptional Profiling of the Adult Hair Follicle Mesenchyme Reveals R-spondin as a Novel Regulator of Dermal Progenitor Function

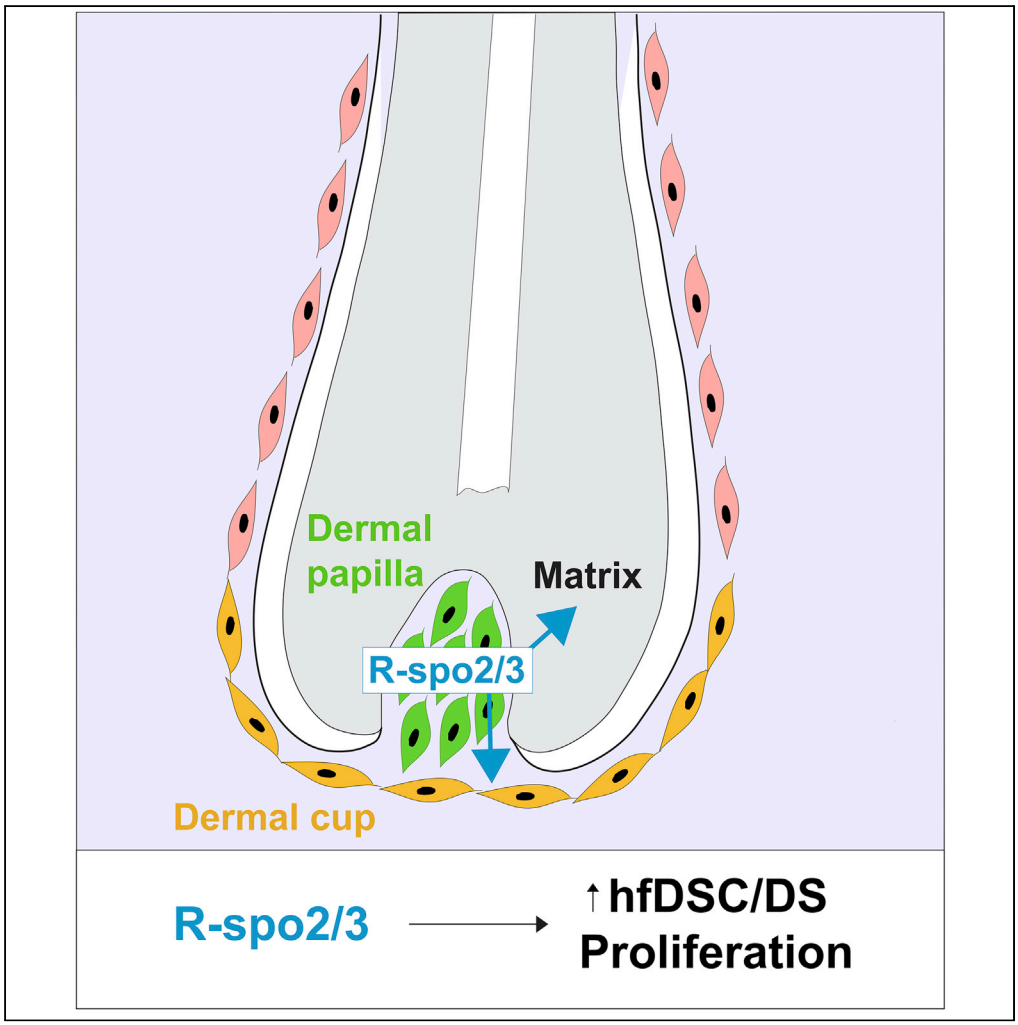

Andrew Hagner, Wisoo Shin, Sarthak Sinha, ..., John Cobb, Ina Dobrinski, Jeff Biernaskie

jeff.biernaskie@ucalgary.ca

HIGHLIGHTS

Transcriptional compartmentalization of the hair follicle mesenchyme

Hair follicle dermal stem cells (hfDSCs) exhibit a unique gene expression profile

DP-derived R-spondins coordinately activate hfDSCs and epithelial progenitors

Gene expression profiling of hair follicle dermal stem cells

DATA AND CODE AVAILABILITY

GSE109256

Hagner et al., iScience *23*, 101019
April 24, 2020
https://doi.org/10.1016/j.isci.2020.101019

iScience

CellPress

Article

Transcriptional Profiling of the Adult Hair Follicle Mesenchyme Reveals R-spondin as a Novel Regulator of Dermal Progenitor Function

Andrew Hagner,[1] Wisoo Shin,[1] Sarthak Sinha,[1] Whitney Alpaugh,[1] Matthew Workentine,[1] Sepideh Abbasi,[1] Waleed Rahmani,[1] Natacha Agabalyan,[1] Nilesh Sharma,[1] Holly Sparks,[1] Jessica Yoon,[1] Elodie Labit,[1] John Cobb,[5] Ina Dobrinski,[1] and Jeff Biernaskie[1,2,3,4,6,*]

SUMMARY

The adult hair follicle (HF) undergoes successive regeneration driven by resident epithelial stem cells and neighboring mesenchyme. Recent work described the existence of HF dermal stem cells (hfDSCs), but the genetic regulation of hfDSCs and their daughter cell lineages in HF regeneration remains unknown. Here we prospectively isolate functionally distinct mesenchymal compartment in the HF (dermal cup [DC; includes hfDSCs] and dermal papilla) and define the transcriptional programs involved in hfDSC function and acquisition of divergent mesenchymal fates. From this, we demonstrate cross-compartment mesenchymal signaling within the HF niche, whereby DP-derived R-spondins act to stimulate proliferation of both hfDSCs and epithelial progenitors during HF regeneration. Our findings describe unique transcriptional programs that underlie the functional heterogeneity among specialized fibroblasts within the adult HF and identify a novel regulator of mesenchymal progenitor function during tissue regeneration.

INTRODUCTION

Owing to its capacity for continuous cyclic growth and degeneration throughout adult life, the hair follicle (HF) provides a powerful model to study stem cell dynamics and molecular cross talk that is required to enable tissue regeneration. Considerable work has focused on the hair follicle epithelial stem cell lineage (Hsu et al., 2011; Joost et al., 2016; Taylor et al., 2000; Tumbar et al., 2004), but our understanding of the supporting mesenchymal cells, their functional diversity, and the molecular signals that regulate their inductive capacity remain poorly understood.

The HF mesenchyme can be divided into three functionally distinct compartments. The dermal papilla (DP) is a small cellular aggregate residing at the base of each HF, which provides signals to initiate and coordinate epithelial progenitor function to enable regeneration (Clavel et al., 2012; Jahoda et al., 1984). Indeed, transplantation of DP is sufficient to induce ectopic hair growth, whereas ablation of the DP impairs HF growth emphasizing the importance of the mesenchymal niche (Jahoda et al., 1984; Rompolas et al., 2012). The connective tissue sheath (CTS; also called the dermal sheath; DS) surrounds the transient regenerative segment of the HF and is contiguous with the DP. The DS compartment can be distinguished by its continuous expression of alpha smooth muscle actin (αSMA). Recent work has described a functional hierarchy within these compartments and the existence of a self-renewing dermal stem/progenitor cells (hair follicle dermal stem cell [hfDSC]) that reside at the anagen dermal cup (DC) and function to populate both DP and the DS at the onset of each new regenerative cycle (Rahmani et al., 2014). hfDSCs can be prospectively isolated from Sox2-expressing cells in the DS and form self-renewing colonies *in vitro* that are able to reconstitute the HF mesenchyme and initiate *de novo* hair follicle formation (Biernaskie et al., 2009; Rahmani et al., 2014). Indeed, understanding the cellular communication that occurs between HF mesenchyme and epithelial cells to enable HF regeneration will have important implications for maintaining skin health or in developing regenerative therapies to better repair damaged skin or to restore hair growth.

To this end, we prospectively isolated hfDSCs and their differentiated progeny from adult skin at the onset of HF regeneration and then performed bulk RNA sequencing (RNA-seq) to establish gene expression signatures for each mesenchymal compartment. Employing both *in vitro* and *in vivo* approaches, we demonstrate inter-compartment mesenchymal signaling during the initiation of hair growth, whereby

[1]Department of Comparative Biology and Experimental Medicine, Faculty of Veterinary Medicine, University of Calgary, Calgary, AB, Canada

[2]Department of Surgery, Cumming School of Medicine, University of Calgary, Calgary, AB, Canada

[3]Alberta Children's Hospital Research Institute, Calgary, AB, Canada

[4]Hotchkiss Brain Institute, University of Calgary, Calgary, AB, Canada

[5]Department of Biological Sciences, University of Calgary, Calgary, AB, Canada

[6]Lead Contact

*Correspondence: jeff.biernaskie@ucalgary.ca

https://doi.org/10.1016/j.isci.2020.101019

R-spondins are secreted from the DP to synchronously stimulate proliferation of both hfDSCs and epithelial progenitors.

RESULTS

Prospective Isolation of Distinct Functional Compartments within the Adult HF Mesenchyme

To begin dissecting the adult mesenchymal lineage within the HF, and to understand the transcriptional programs that underlie their distinct functions within each mesenchymal compartment (Figure 1A), we generated αSMA^{dsRed}:$Sox2^{GFP}$ mice to enable prospective identification of each mesenchymal compartment. This included hfDSCs that reside in the most proximal region of the DS of anagen HFs (called the dermal cup). DC cells that include hfDSCs are uniquely identified by their co-expression of αSMA and Sox2 (αSMA^{dsRed+}:$Sox2^{GFP+}$; Figures 1B and 1E), whereas the DP exhibits only *Sox2* expression (Biernaskie et al., 2009; Chi et al., 2015, Driskell et al., 2009; Figure 1B). Arrector pili muscle cells (which also express αSMA) were excluded based on their robust expression of ITGα8 ($ITG\alpha8^{Hi}$). DP cells were identified as $\alpha SMA^{dsRedNEG}$/$Sox2^{eGFP+ve}$ and further enriched by collecting the $ITG\alpha9^{+ve}$ fraction, which marks DP cells (Figures 1B–1F) but excludes cutaneous glial cells that also express SOX2 (Biernaskie et al., 2009; Clavel et al., 2012). As a comparative population of non-hair follicle dermis, $\alpha SMA^{dsRedNEG}$/$Sox2^{eGFPNEG}$/$ITG\alpha8^{NEG}$ cells were also collected, which are hereafter referred to as the interfollicular dermis (IFD; Figure 1G). Additional staining can be found in Figure S1.

Gene Expression Analysis Reveals Distinct Molecular Signatures for hfDSCs and Their Progeny

RNA-seq libraries were generated for each sample cell population (n = 3/population): DC, DP, and IFD. Each replicate sample originated from different litters of mice and contained pooled samples of two to five mice in order to collect sufficient number of cells and obtain high-quality RNA. Principle component analysis (PCA) identified three distinct cell populations with clustered replicates (Figure 2A). All populations (DC, DP, and IFD) exhibited low variation between replicates and showed unique gene expression profiles. Commonalities across mesenchymal compartments is shown as a Euler plot in Figure 2B.

To begin to understand the molecular regulators that define the unique fate and functions ascribed to each of these adult fibroblast subtypes, we developed genetic signatures for each compartment. Signatures were defined as transcripts exhibiting a $\geq$2-fold differential upregulation (FPKM > 5; adjusted p value <0.05), in comparison with the other mesenchymal cell populations (Figure 2C). Lists of the 50 most differentially expressed upregulated signature genes from each HF mesenchymal compartment are shown in Figure 2D. The combined gene expression of DC and DP populations generated the signature gene list of HF mesenchyme (HFM; in comparison to IFD; Figure 2D). Gene ontology analysis identified several important functional themes for each mesenchymal compartment (Figure 2E). Interestingly, the DC signature was associated with regulation of cell-cell adhesion, actin-based cell projections, and cytoskeleton components (Figure 2E), which may encompass dividing cells as well as differentiation to mature dermal sheath fates. The DP compartment was highlighted by regulation of hair cycle, growth factor activity, intracellular receptor signaling pathways, and neuron recognition/neurotransmitter activity (Figure 2E). As a whole, the HF mesenchyme signature was most notably associated with *Bmp* binding (Figure 2E), which is a well-documented pathway involved in the HF regeneration cycle (Kobielak et al., 2003; Rendl et al., 2008).

Validation of Identified Signature Genes within the HF Mesenchyme

Differential expression of identified genes from each compartment was validated through TaqMan quantitative-PCR (Figures 3A–3C), immunohistochemistry (Figures 3D–3H), and RNAScope (Figures 3I–3M). Candidate genes were chosen based on enrichment within a singular compartment and expressing (1) previously demonstrated cellular markers, (2) transcription factors that might regulate cell proliferation, (3) ligands-related stem cell signaling, or (4) extracellular receptors. qPCR was performed in biological and technical triplicate, using samples that were entirely distinct from those used for RNA-seq. RNA-seq log2-fold change in gene expression of the selected signature genes was highly correlated (r = 0.78; Figure 3A) with that of the qPCR demonstrating the validity of our data. From this, we identified several novel or signature genes associated with each mesenchymal compartment. Within DC we validated expression of *Epha3*, *Hic1*, *Itgα11*, *Igbfp2*, *Mcam*, *Pcp4*, *Pdgfrl*, and *Tnnt1* (Figure 3B). For DP, we confirmed

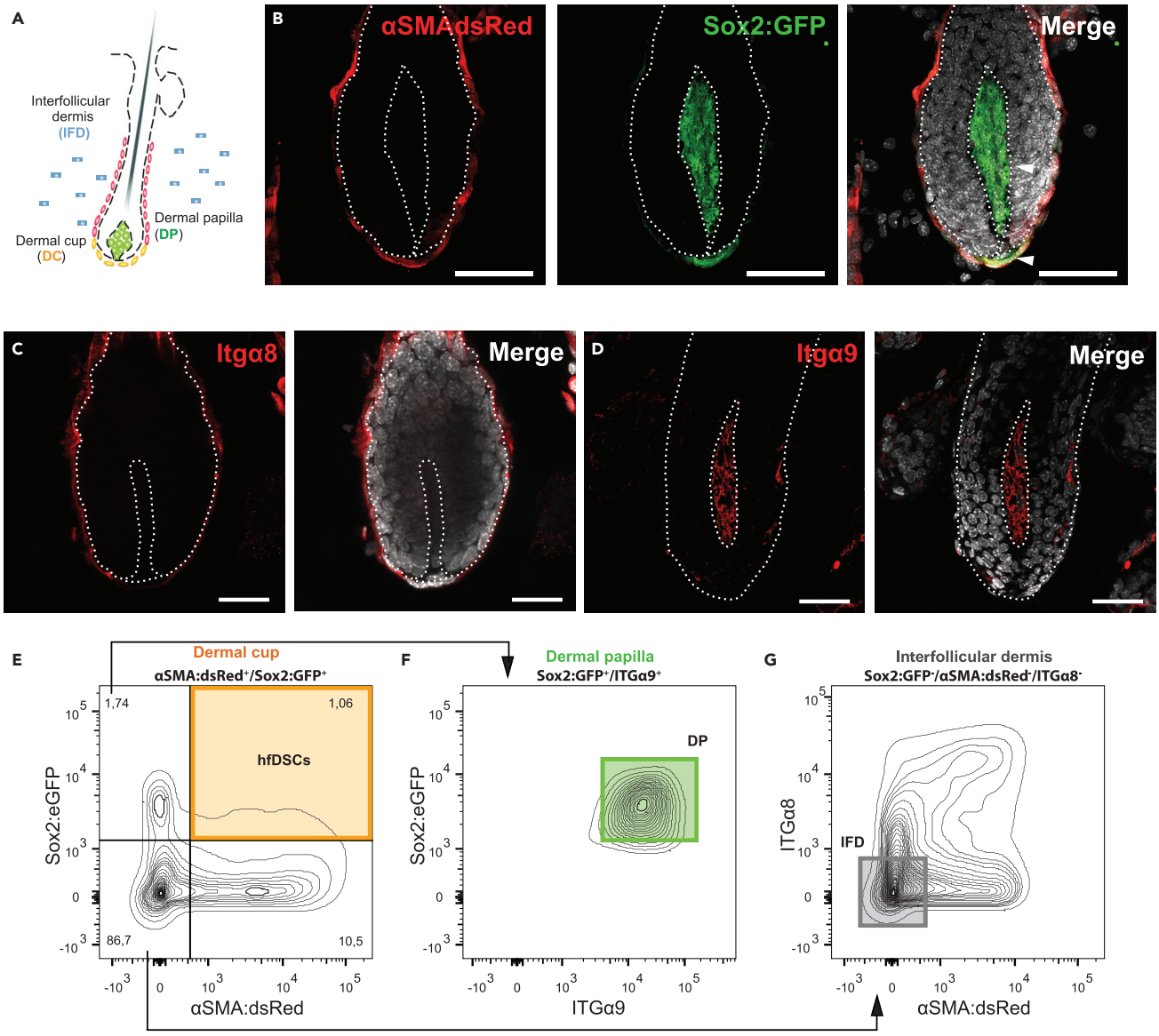

Figure 1. Prospective Isolation and Transcriptomic Analysis of hfDSCs and Their Progeny within the Regenerating Adult Hair Follicle

(A) Schematic of adult anagen hair follicle. Functionally distinct mesenchymal compartments are indicated by an identifiable name and color.

(B) Images of early anagen hair follicle bulbs on adult αSMA^{dsRed}:Sox2^{GFP} double knockin mice stained with Hoechst (gray). Sox2^{GFP} is expressed in the DP (green; upper arrow), whereas the DC (yellow; lower arrow) is both αSMA^{dsRed} and Sox2^{GFP} positive. Scale bar, 100 μm.

(C and D) Images showing immunostaining for (C) Itgα8 (red) and (D) Itgα9 (red) labeling the dermal sheath and dermal papilla, respectively. Hoechst identifies cell nuclei (gray). Scale bar, 50 μm.

(E–G) FACS isolation and gating strategy used to isolate (E) DC, (F) DP. and (G) IFD. Representative contour plots indicate each specific mesenchymal compartment within the hfDSC lineage.

the expression of *Fgf7*, *Hey2*, *Pax1*, *Prlr*, *Rspo3*, *Sostdc1*, and *Vcan* (Figure 3C). Given the marked elevation of Rspo3 in the DP, we re-examined Lgr receptor expression in our RNA-seq data and found that transcripts for each were largely present in DP, DC, and IFD (Figure 3D). Using immunofluorescence we confirmed the presence of encoded protein for *Vcan*, *Runx3*, and *Rspo2* within the DP (Figures 3E–3G) as well as *Itgα5* and *CD200* (Figures 3H and 3I), both of which are novel membrane receptors corresponding to the murine DC. Using RNAScope, we validated the presence of *Rspo3* and *Spock3* mRNA in the DP (Figures 3J and 3K) and *Adamts18* and the *Rspo* receptor *Lgr6* mRNA in the DC (Figures 3L and 3M). Interestingly, unlike *Lgr6*, expression of *Lgr4* mRNA appeared restricted to the HF epithelium

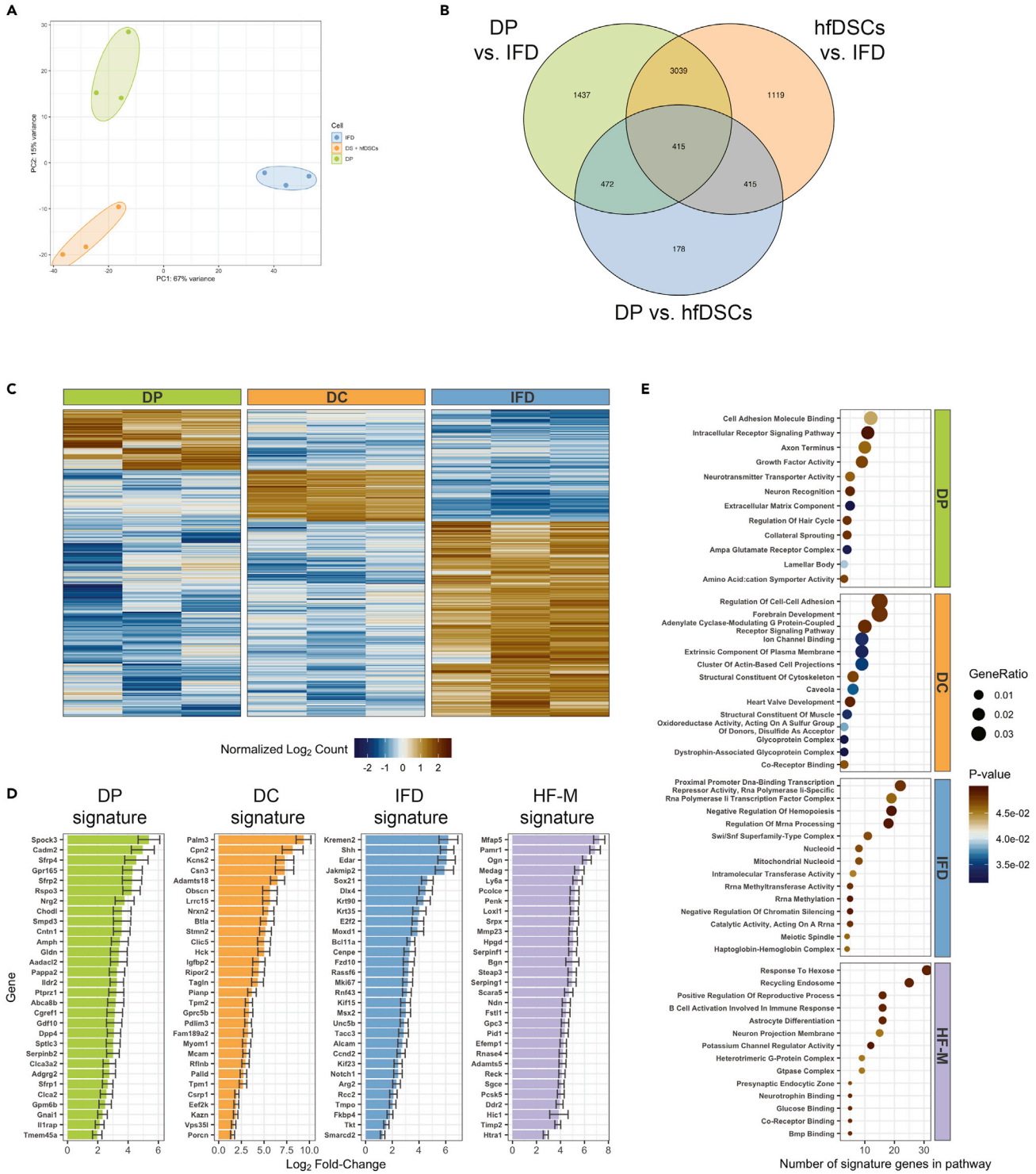

Figure 2. RNA-Seq Analysis Reveals a Distinct Molecular Signature for Each Hair Follicle Mesenchymal Compartment

(A) Principal component analysis (PCA) of global gene expression profiles of DC, DP, and IFD comparing PC1 and PC2. Component percent contribution to variance is noted in each axis title.

(B) Modified Euler diagram depicting numbers of differentially expressed genes in each cell population comparison with ≥2-fold differential gene expression.

Figure 2. *Continued*

(C) Heatmap representation of identified signature genes (log_2 FPKM) for DP, DC, and IFD during early anagen. Each row represents expression for a single gene, and columns indicate biological replicates grouped by population. DP, dermal papilla; DC, dermal cup; IFD, interfollicular dermis.

(D) Compound graphs depicting the top 50 most significant differentially expressed genes ranked by fold change. Bars show mean log2-fold change between indicated cell populations compared with the other populations ($\pm$SEM, $q \leq 0.05$). The hair follicle mesenchyme (HF-M) population is the mixed gene expression of DC and DP compared with the IFD.

(E) Gene ontology analysis of biological and molecular processes for signature genes in DP, DC, IFD, and HF-M.

and not the DC or CTS (Figure 3N). Images showing positive and negative control probes are provided for comparison (Figures 3O and 3P).

Regulators of Inductive Function and Mesenchymal Cross Talk

Although signatures for the developing neonatal DP have been described (Rendl et al., 2005; Rezza et al., 2016; Sennett et al., 2015), a comprehensive transcriptional profile for the adult early anagen DP is lacking. We therefore compared our DP signature with previously published "core" neonatal anagen DP genes and found 54 enriched transcripts in common (Figure S2A and S2B). To further define the transcriptional programs associated with inductive competency, we generated a list of shared transcripts showing the highest level of expression between hfDSC and DP compartments, and differentially expressed compared with interfollicular dermal fibroblasts (IFD), which might also include upper dermal sheath cells, but neither of which exhibit inductive function (McElwee et al., 2003; Figure S2D). These genes included *Ogn*, *Timp2*, *CD248*, *Pcolce*, *Dpt*, *Timp1/2*, *Serping1*, *Clec3b*, *Ly6a*, *Hic1*, *Ccl8*, *Pi16*, and others (Table S1 for complete lists). We also probed potential receptor-ligand interactions that may underlie cross talk between the mesenchyme and adjacent melanocytes, keratinocytes comprising the matrix cells, and hair germ/transit-amplifying cells (TACs) (Hsu et al., 2014), as well as potential inter-compartmental communication between mesenchymal cells (Figure S3). DP cells are enriched for ligands *Edn3* and *Nrg2*, which bind to melanocyte receptors *Ednrb* and *Erbb4*, genes related to melanocyte differentiation. DP cells also express the Hedgehog signaling pathway antagonist, *Hhip*, which interacts with the morphogen *Shh*, secreted by transit-amplifying cells (TACs), shown to be necessary for adult HF cycling (Wang et al., 2000). Furthermore, DP cells express the ligand *Aloxe3*, which can be cross-linked by the membrane-bound enzyme *Tgm1* on nearby matrix/TACs to facilitate epithelial cell differentiation. Potential inter-mesenchymal cross talk is indicated by expression of ligand/receptor pairings such as *Dcc/Ntn1* and *Edn3/Ednr(a/b)* between DP cells and hfDSCs. Our adult mouse DP signature gene list was also compared with other published mouse DP signature lists to determine definitive DP genes that are conserved across hair types and from embryogenesis to adulthood (Figures S2A–S2D) (Rendl et al., 2005; Rezza et al., 2016; Sennett et al., 2015). Essential DP genes include *Chodl*, *Crabp1/2*, *Edn3*, *Fgf7/10*, *Hhip*, *Itga9*, *Pappa*, *Rspo2-4*, *Serpine3*, and *Sfrp1/2* (Figures S2B and S2D). Of particular note are the genes conserved between mouse and human DP, when compared with previous microarray data (Higgins et al., 2013; Ohyama et al., 2012) (Figures S2E and S2F). Our DP signature shared 28 genes in common with these previous signatures. One example was *Gpx3*, which serves to protect cells from oxidative stress by catalyzing the reduction of hydrogen peroxide and hydroperoxides and has been reported as a downstream target of thyroid-stimulating hormone signaling in HF fibroblasts (Bodo et al., 2009). *Dio2* was also identified and similarly catalyzes production of bioactive thyroid hormone and has also been reported as a signature gene for human HF bulge stem cells (Ohyama et al., 2006). Conserved DP signature genes between human and mouse include *Chodl*, *Crabp1*, *Dio2*, *Edn3*, *Gpm6b*, *Gpx3*, *Hhip*, *Pappa2*, *Rspo2*, *Sfrp1/2*, *Sostdc*, and *Sparcl1* (Figure S2F).

R-spondin2/3 Promotes Proliferation of Isolated hfDSCs

Specific components of the Wnt-signaling pathway were highly enriched throughout the adult HF mesenchyme (Figures 2D and S2B). Most notable was the robust compartment-specific expression of all four R-spondin ligands within the DP (also observed in neonatal DP; Rendl et al., 2005; Rezza et al., 2016; Sennett et al., 2015) (Table S1). R-spondins are potent Wnt enhancers and play a critical role in regulating somatic stem cells in several organs including epithelial stem/progenitors in the HF and intestinal crypt (Abo and Clevers, 2012). Intriguingly, our transcriptomic dissection of the mesenchyme also revealed expression of R-spondin receptors *Lgr4/5/6* in neighboring DC cells as well as in IFD (Figure 3D; Table S1). All other data supporting the findings of this study are available from the corresponding author upon request. Indeed our *in situ* hybridization on early anagen skin validated the expression of *Lgr6*, but not *Lgr4*, within the DC and neighboring epithelial matrix (Figures 3M and 3N). One recent

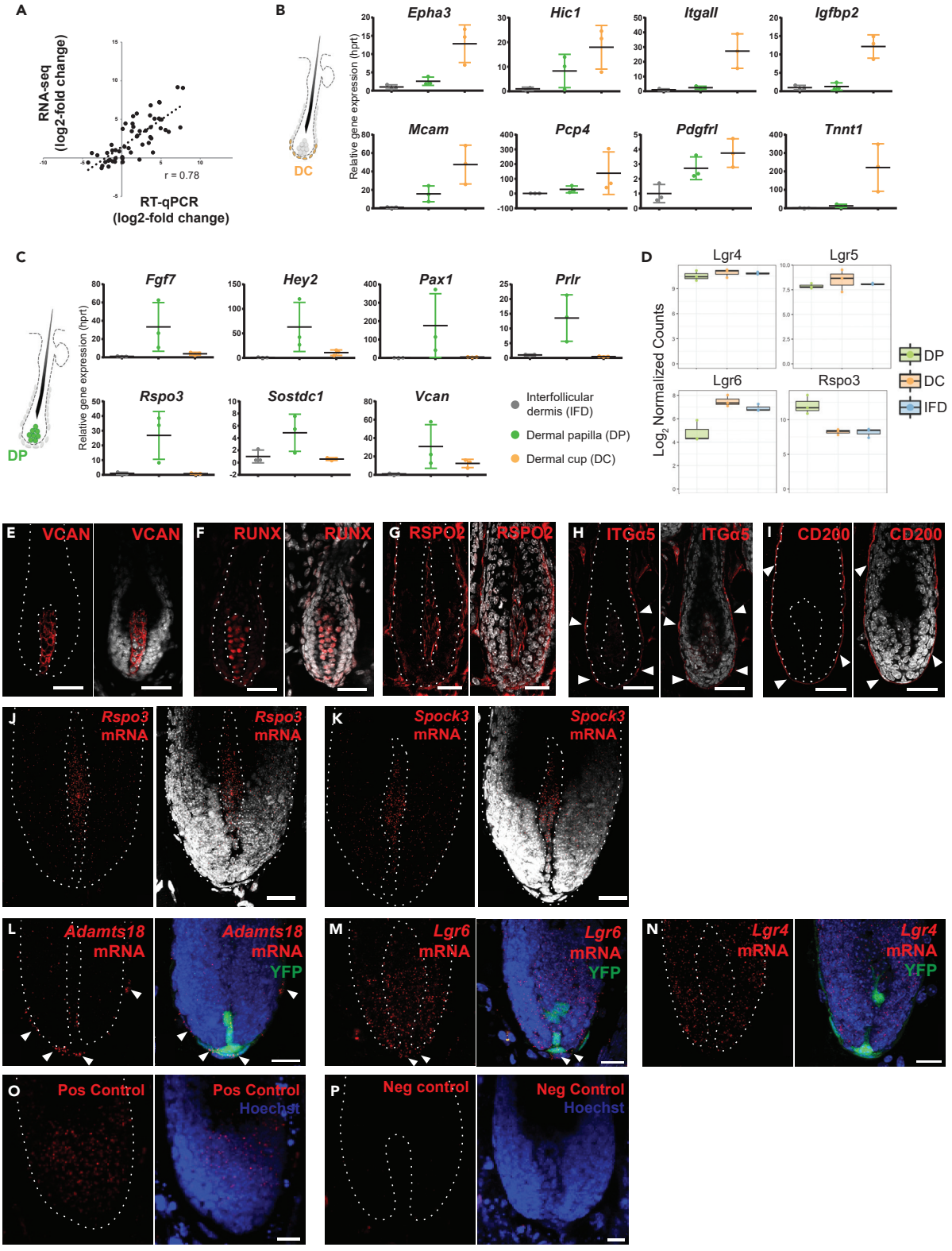
A
RNA-seq (log2-fold change)
RT-qPCR (log2-fold change)
r = 0.78
B
DC
Relative gene expression (hprt)
Epha3
Hic1
Itgall
Igfbp2
Mcam
Pcp4
Pdgfrl
Tnnt1
C
DP
Relative gene expression (hprt)
Fgf7
Hey2
Pax1
Prlr
Rspo3
Sostdc1
Vcan
Interfollicular dermis (IFD)
Dermal papilla (DP)
Dermal cup (DC)
D
Lgr4
Lgr5
Lgr6
Rspo3
Log2 Normalized Counts
DP
DC
IFD
E VCAN VCAN
F RUNX RUNX
G RSPO2 RSPO2
H ITGα5 ITGα5
I CD200 CD200
J Rspo3 mRNA Rspo3 mRNA
K Spock3 mRNA Spock3 mRNA
L Adamts18 mRNA Adamts18 mRNA YFP
M Lgr6 mRNA Lgr6 mRNA YFP
N Lgr4 mRNA Lgr4 mRNA YFP
O Pos Control Pos Control Hoechst
P Neg control Neg Control Hoechst

Figure 3. Validation of Candidate Genes in Mouse Skin Reveals Compartment-Specific Markers within the Hair Follicle Mesenchyme

(A) Spearman correlation of log2-fold change values from RNA-seq and subsequent qPCR ($r = 0.78$, $P < 0.0001$, Spearman correlation coefficient).

(B and C) TaqMan RT-qPCR results for candidate gene expression for each HF mesenchymal compartment relative to the endogenous control gene *hprt*. Each gene was tested in technical and biological triplicate (only biological replicates shown), using samples collected independently of those used for RNA-seq. Genes are grouped by mesenchymal compartment; (B) DC and (C) DP. Data are mean ± SD.

(D) Log2 normalized counts of Lgr4, Lgr5, Lgr6, and Rspo3 in DP, DC, and IFD. Levels of Lgr4, Lgr5, and Lgr6 are detected in the DC. Data are mean log2 normalized counts ± SD, n = 3 biological replicates.

(E–I) Immunohistochemistry of candidate genes in early anagen (~P26) mouse back skin. Images show hair follicle bulbs with DS and DP outlined. Hoechst nuclear staining in gray and immunostaining in red. (E) Versican (Vcan), (F) Runt-related transcription factor 1-3 (Runx), (G) R-spondin2 (Rspo2), (H) Integrin alpha 5 (Itgα5), and (I) CD200. (H, I) Arrowheads indicate staining of DS and DC. Scale bars, 50 μm.

(J and K) RNAScope of candidate genes in early anagen (P26) mouse back skin. Images show hair follicle bulbs with DS and DP outlined. Hoechst nuclear staining in gray and mRNA in red. (J) *Rspo3* mRNA; (K) Spock3 mRNA. Scale bars, 50 μm.

(L–N) RNAScope of candidate genes in early anagen (P26) αSMACreER^{T2}:Rosa^{eYFP} mouse back skin treated with tamoxifen at p3/4. The details of this mouse can be found in Transparent Methods. Images show hair follicle bulbs with DS and DP outlined. Hoechst nuclear staining in blue, mRNA in red, and YFP in green. (L) Adamts18 mRNA; (M) Lgr6 mRNA; (N) Lgr4 mRNA. (L and M) Arrowhead indicates respective mRNA-positive cells in the DC. Scale bars, 50 μm.

(O and P) RNAScope of (O) positive control (Ubiquitin C) and (P) negative control (DapB) gene from *Bacillus subtilis* strain SMY in early anagen (P26) mouse back skin. Images show anagen hair follicle bulbs with the hair follicle outlined in white. Hoechst nuclear staining is in blue and mRNA is in red. Scale bars, 25 μm.

study showed that exogenous application of recombinant RSPO2 is sufficient to prolong the anagen cycle (Smith et al., 2016); however, the source of R-spondins and their impact on mesenchymal cell function, particularly during tissue regeneration, remain unknown. By immunostaining for RSPO2 protein, we found discrete labeling of the early anagen DP (Figure 4A) corroborating our RNA-seq data. Given that the R-spondin receptor *Lgr6* is present in the DC (Figure 3L), we asked whether R-spondin might act as an intra-mesenchymal modulator of hfDSC function in addition to its previously described role in mesenchymal-epithelial cross talk. To test this, we isolated αSMA$^{dsRed+ve}$ Sox2^{GFP+ve} ITGα8^{lo} hfDSCs from the DC (Figure 4B) and grew them *in vitro* at clonal density in the presence or absence of recombinant RSPO2/3 or in combination with the small molecule *Wnt* activator, CHIR99021 (CHIR) (Figure 4C). As an additional control, we compared exposure to TGFβ2, a known inducer of anagen (Oshimori and Fuchs, 2012).

Growth in either RSPO2/3 or CHIR alone displayed a >2-fold increase in mean colony number (Figure 4D), whereas a combination of RSPO2/3 and CHIR was additive, exhibiting a >3-fold increase in the number of colonies per well. TGFβ2 showed only a modest increase in colony number and a negligible increase in colony size (Figures 4E–4G). Further analysis of binned colony sizes showed that RSPO2/3 increased total number of colonies and frequency of large colonies (Figure 4E) and increased the overall average colony size and number (Figures 4F and 4G) indicative of enhanced proliferation. Since Lgr receptors are also expressed in the telogen hair germ/bulge and anagen matrix (Figures 3L and 3M), we postulated that epithelial keratinocytes may also be activated by R-spondin signaling. Primary mouse keratinocytes were dissociated from isolated neonatal hair follicles and plated in the presence of RSPO2 or 3. Both RSPO2 and 3 elicited a nearly ~30% increase in the size of keratinocyte colonies relative to parallel control cultures (Figures 4H and 4I). Together, these results suggest that both Rspo2 and 3 are sufficient to induce proliferation of both mesenchymal and epithelial progenitors.

We next asked whether RSPO2 and RSPO3 have a redundant or additive effect on isolated hfDSCs. Isolated hfDSCs were treated with RSPO2/3 separately and concurrently (Figure S4). Treatment of either RSPO2 or RSPO3 alone increased the total colony number and final cell number to comparable degree, but there was no additive effect observed when cells were exposed to RSPO2 and RSPO3 in combination (Figures S4A–S4D). This suggests that the growth-stimulating effects of RSPO2 and RSPO3 are redundant *in vitro*.

To determine whether RSPO3 induces its proliferative effects through the canonical Wnt signaling, isolated cells were treated with DKK1, a known inhibitor of Wnt signaling (Niida et al., 2004) in the presence or absence of RSPO3. Addition of DKK1 mitigated the increase in colony formation observed with RSPO3 treatment (Figures S4–S4G). In parallel, we also blocked Wnt signaling by adding a cocktail of two small molecule inhibitors of the Wnt pathway (IWP2 and IWR1-endo) (Chen et al., 2009) and similarly showed that it was sufficient to block the growth potentiation provided by RSPO3 (Figures S6H–S6I).Together these data suggest that stimulation of hfDSC by R-spondin signaling occurs via the canonical Wnt-signaling pathway.

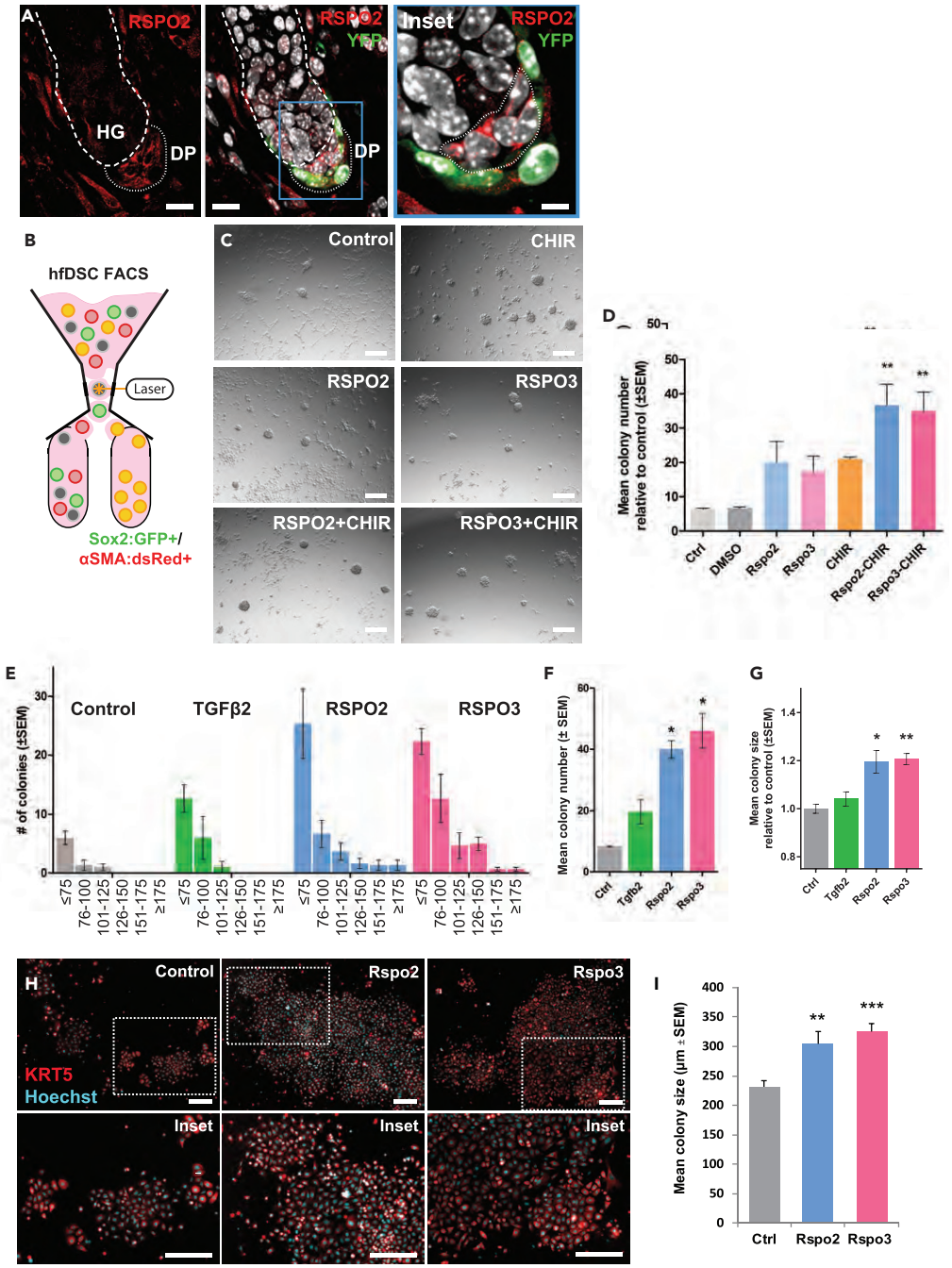

Figure 4. R-spondins-2 and -3 Stimulate Proliferation of Prospectively Isolated hfDSCs and Hair Follicle Keratinocytes

(A) Early anagen follicle from α-SMACreER^{T2}:Rosa^{eYFP} skin showing Rspo2 (red) in DP cells, surrounded by hfDSCs (green). High magnification inset (blue box) shown at right. HG, hair germ. Scale bar, 10 μm.

(B) Schematic showing FACS isolation of hfDSCs (αSMAdsRed^{+ve} Sox2GFP$^{+ve)}$ from anagen (P26) skin.

(C) Phase contrast images of isolated hfDSCs grown for 10 days in the absence or presence of recombinant mouse Rspo2 or 3 protein and/or the GSK-inhibitor CHIR99021 (D). Scale bar, 50 μm.

(D) Quantification of hfDSC colony numbers. Experiments included no treatment and DMSO only controls. Mean ± SEM (n = 3 biological replicates, ** indicates P ≤ 0.01).

(E) Distribution of colony sizes following exposure to DMSO, TGFβ2, RSPO2, or RSPO3. Data are mean ± SEM.

Figure 4. *Continued*

(F and G) Quantification of colony (F) number and (G) size of FACS-isolated hfDSCs grown in equivalent conditions, with the addition of TGFβ2, RSPO2, or RSPO3 treatment. Data are mean ± SEM (n = 3 biological replicates; *, $p \leq 0.05$, **$p \leq 0.01$).

(H) Adult (p26) epithelial keratinocytes grown for 10 days in the absence or presence of recombinant mouse RSPO2 or RSPO3 protein and immunostained with Keratin-5. Scale bar, 50 μm.

(I) Quantification of mean keratinocyte colony size from (H) (mean ± SEM, n = 3 biological replicates, **, *** indicate $p \leq 0.01$, 0.001, respectively).

Exogenous R-spondin Is Sufficient to Induce Precocious Anagen and Depletion of Rspo3 within DP Delays HF Growth

To test the sufficiency of RSPO2/3 to activate HF stem/progenitors toward initiation of HF regeneration *in vivo*, we performed intradermal injections of RSPO2 or 3 into resting telogen skin (P55). Controls included injection of either TGFβ2, a known inducer of anagen (growth), or BSA vehicle. Unsurprisingly, vehicle control injections remained in resting phase (telogen) for the duration of the 4-week experiment (Figure 5A). In contrast, application of either RSPO2 or RSPO3 initiated a rapid onset of anagen hair growth (Figures 5C and 5D) that was indistinguishable from injection of TGFβ2 (Figure 5B).

To determine the functional importance of DP-derived *Rspo3* in regulating hfDSCs and HF regeneration *in vivo*, we generated Prominin1CreER^{T2}:*Rspo3*$^{flox/flox}$ mice (Figure 5E). *Prominin-1* (*CD133*) is enriched in DP cells, thereby allowing specific deletion of *Rspo3* within the DP compartment (Zhou et al., 2016). Tamoxifen was applied at either postnatal day 2–4 (Figure 5F) or at the onset of the second anagen (P20–24) (Figure 5G). In either experiment, conditional depletion of *Rspo3* (*Rspo3*$^{-/-}$) within the DP resulted in delayed natural hair regrowth relative to *Rspo3*$^{+/+}$ controls after tamoxifen injection (Figures 5F and 5G). The distribution of HF stages was markedly altered in *Rspo3*$^{-/-}$ showing the majority of HFs remaining in early or mid anagen, whereas *Rspo3*$^{+/+}$ mice had a majority of late anagen HFs (Figures 5H and 5I). The knockdown efficiency of Rspo3 in Prom1+ cells was confirmed through qPCR (Figure 5J). To verify the specificity of *Rspo3* within the DP, we generated αSMACreER^{T2}:*Rspo3*$^{flox/flox}$ mice, where *Rspo3* was conditionally deleted from DC, but not the DP. Here, we did not observe any changes in HF growth over two consecutive depilation induced cycles (Figure S4; n = 3 per genotype), demonstrating that *Rspo3* is derived specifically from the mesenchymal cells residing in the DP and not other mesenchymal cells. These results show that DP-derived R-spondins are sufficient to initiate progenitor activation and HF regeneration during competent telogen but are not required for initiation of HF regeneration.

R-spondin Enhances Proliferation of Isolated Adult Human Dermal Progenitors *In Vitro*

To begin to translate our findings to human dermal fibroblast biology, we performed immunofluorescence staining on adult human scalp skin sections and confirmed the presence of several identified transcripts. In the human anagen DP, we observed robust expression of candidate genes *Runx* and *Vcan* (Figures 6A and 6B). *Pax1* and *Bgn* was found in the human DC (Figures 6C and 6D). Immunostaining of RSPO2 confirmed enrichment in the DP and DC, with expression in the epithelium as well (Figure 6E). To determine whether R-spondins act as instructive signals for human mesenchymal progenitors, we performed colony formation assays on primary adult human dermal progenitors in the presence or absence of R-spondin2/3 for 14 days (Figure 6F) and observed a >3-fold increase in colony number and a 20%–40% increase in colony size (Figures 6G and 6H). Lastly, immunostaining confirmed the presence of LGR4, suggesting that RSPO2/3 may act directly on human dermal progenitors (Figure 6I). Next, the cultured dermal progenitors were pulsed with BrdU at passage 2 (day 5) for 18 h and BrdU uptake was quantified by flow cytometry (Figure 6J) to determine whether RSPO3 similarly enhances proliferation of human dermal progenitors. Gating for BrdU fluorescence intensity was identified with positive and negative controls, and the same settings were used to quantify the percentage of cells undergoing DNA replication (0, 1, or 2 times) during the 18-h pulse period (Figures 6K and 6L). Indeed, the largest proportion of cells in the control cultures had completed one replication cycle, whereas the majority of cells in the RSPO3-treated cultures had initiated a second cycle (Figure 6M) suggesting that RSPO3 may accelerate the rate of cell cycling. Lastly, to determine whether R-spondins may be influencing the number of proliferating cells or preventing cell death, flow cytometry was used to quantify the percentage of proliferating (Ki67^{+}) and apoptotic (Casp3^{+}) cells after RSPO3 or RSPO3 + CHIR treatment (S6A). Indeed, there was a modest but significant increase in *Ki67*$^{+}$ cells (Figures S6B and S6D) and also a similar increase in apoptotic *Casp3*$^{+}$ cells (Figures S6C and S6E) suggesting that neither RSPO3 or CHIR treatments impact cell survival. Notably, there was an increase in the total

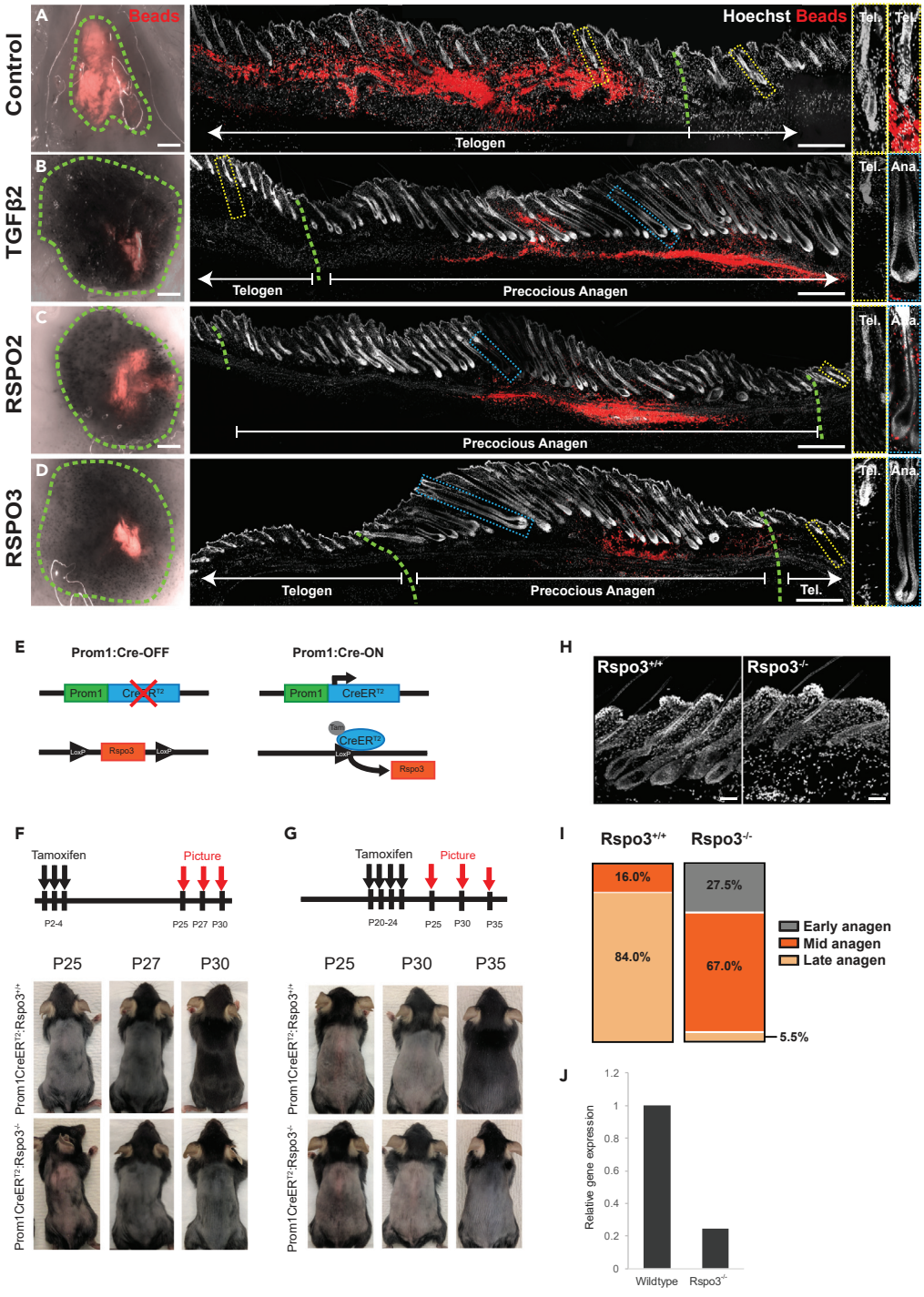

Figure 5. Exogenous R-spondin 2/3 Is Sufficient to Stimulate Hair Follicle Regeneration *In vivo* and Deficiency in DP-Derived R-spondin 3 Delays Progression of Anagen

(A–D) Images of skin following intradermal injection of (A) BSA, (B) TGFβ2, (C) RSPO2, and (D) RSPO3 into resting phase (telogen) adult mouse back skin. At left are ventral views of skin at each injection site. Red indicates fluorescent beads used to identify injection site. In the main panel, nuclei are stained with Hoechst (gray). Green dashed lines outline the injection site. Dashed boxes (yellow, telogen; blue, anagen) indicate high magnification insets of individual follicles shown at right.

(E) Schematic depicting Prominin-1CreER^{T2}:*Rspo3*^{flox} mice used to specifically delete *Rspo3* from the dermal papilla.

Figure 5. *Continued*

(F and G) Mice were treated with tamoxifen (4-OHT) at either P3-4 (F; n = 3 of each genotype) or at P20-24 (G; n = 4 of each genotype) to induce recombination. Representative images show hair regrowth in either *Rspo3*$^{+/+}$ (top) or *Rspo3*$^{flox/flox}$ mice (bottom).

(H) Cross section of P30 Rspo-3$^{+/+}$ (top) and *Rspo3*$^{flox/flox}$(bottom) mouse skin stained with nuclei labeled with Hoechst (gray). Mice were treated with 4-OHT at P2-4, 20, 21.

(I) Quantification of the percentage of HF in early, mid-, or late anagen for *Rspo3*$^{+/+}$ (left; n = 4) and *Rspo3*$^{flox/flox}$ (right; n = 2) mice back skin. Chi-squared distribution analysis was used to compare the difference between HF stage distribution of *Rspo3*$^{+/+}$ and *Rspo3*$^{flox/flox}$ mice ($\chi 2 = 1187$, DF = 2, $p < 0.0001$, two-tailed).

(J) qPCR was performed on mid-anagen (P30) DP cells FACS-isolated by staining for CD133/Prom-1. *Rspo3* gene expression data are relative to an Hprt endogenous control gene. Data are from one experiment with n = 3 independent replicates pooled within each wild-type and *Rspo3*$^{flox/flox}$ groups.

number of cells after RSPO3 + CHIR treatment (Figure S6F). Taken together, the data suggest that R-spondin signaling is sufficient to stimulate proliferation of both rodent and human HF mesenchymal progenitors.

ITGA5 Marks the Connective Tissue Sheath and Enables Prospective Enrichment of Human Dermal Progenitors

Lastly, we examined several extracellular proteins identified within the DC/hfDSC signature to determine whether these could be used to prospectively identify dermal progenitors in adult human skin. We found that, similar to its expression in mouse DC, ITGα5 was also highly enriched in human HF DC and CTS (Figure 7A) with modest expression in the lower DP. Expression of ITGα5 was also found in the HF upper sheath (Figure 7B) but not in the neighboring IFD (Figures 7C and 7D). To determine whether this could be used as a prospective marker, adult human scalp skin was dissociated into single cells, then viable ITGα5^{-} and ITGα5^{+} were collected via fluorescence-activated cell sorting (FACS) and grown in proliferation media for two passages alongside unsorted human progenitor cells (Figures 7E–7G). Both unsorted and ITGα5^{+} fractions exhibited robust clonal colony formation over serial passages, whereas ITGα5^{-} cells failed to generate any colonies (Figures 7H and 7I). Taken together, this suggests that the dermal stem/progenitor population with the adult human dermis is largely contained within the ITGα5-expressing population, which is largely represented by the HF DC/CTS.

DISCUSSION

Our molecular dissection of the adult HF mesenchyme provides new insight into the transcriptional programs that underlie the functional diversity among fibroblast populations within the adult skin. We provide a novel transcriptional characterization of the hfDSC lineage; this includes its resident stem cell pool (hfDSCs in the DC) and a DP signature during the onset of adult HF regeneration, which complements existing knowledge of the neonatal DP (Rendl et al., 2005; Rezza et al., 2016; Sennett et al., 2015). We show that R-spondins stimulate proliferation of epithelial progenitors and hfDSCs *in vitro* and *in vivo* within the HF niche, suggesting that R-spondins may serve to initiate synchronous activation of epithelial and mesenchymal HF regeneration.

One of our most intriguing findings was that secreted factors emanating from the DP not only modulate adjacent epithelial progenitor function but also provide reciprocal signaling to neighboring mesenchymal progenitors (hfDSCs). R-spondins are a family of secreted proteins that act as potent enhancers of Wnt signaling. In the presence of Wnt ligands, R-spondins bind the leucine-rich repeat-containing G-protein-coupled receptors, LGR4–6, and inhibit the Wnt regulators RNF43 and ZNRF3 (Carmon et al., 2011, 2012; de Lau et al., 2014; Ruffner et al., 2012), ultimately preventing degradation of β-catenin and prolonging Wnt activation. Previous studies have described a role for R-spondins in various epithelial stem cell niches such as the HF, small intestine, colon, and stomach (Barker et al., 2007, 2010; Jaks et al., 2008; van der Flier and Clevers, 2009). Indeed, treatment of Lgr5+ bulge epithelial and intestinal crypt cells with Rspo1 had a potent effect on cell proliferation (Jaks et al., 2008; Sato et al., 2009). Here, we found a similar effect in isolated epithelial keratinocytes and demonstrate that R-spondins induce a similarly robust effect on proliferation and self-renewal of prospectively isolated hfDSCs. We propose that the DP secretes R-spondins to synchronously instruct activation of bulge/hair germ progenitors and neighboring hfDSCs in order to enable coordinated HF regeneration.

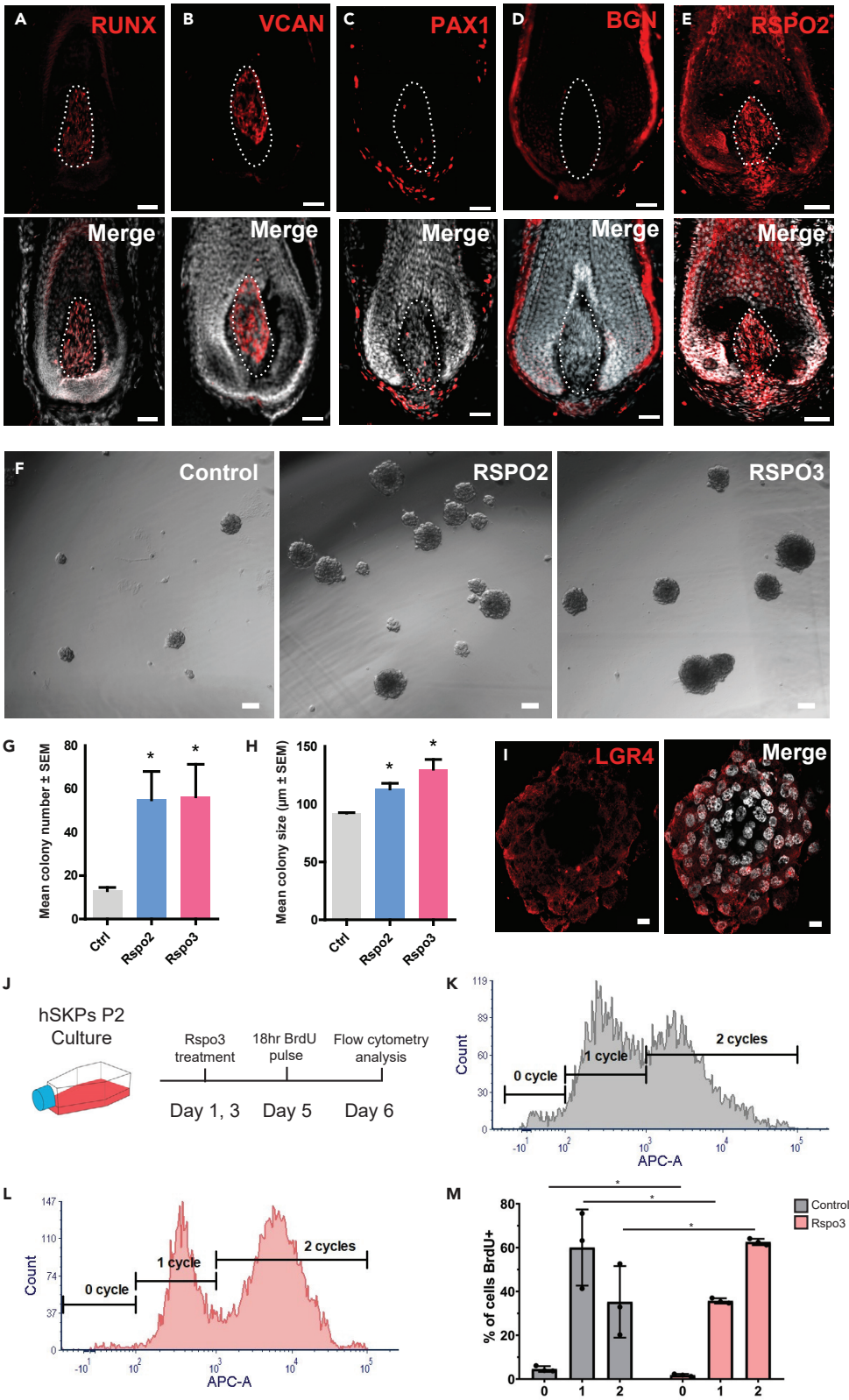
A
RUNX
B
VCAN
C
PAX1
D
BGN
E
RSPO2
Merge
Merge
Merge
Merge
Merge
F
Control
RSPO2
RSPO3
G
Mean colony number ± SEM
80
60
40
20
0
Ctrl
Rspo2
Rspo3
H
Mean colony size (µm ± SEM)
150
100
50
0
Ctrl
Rspo2
Rspo3
I
LGR4
Merge
J
hSKPs P2
Culture
Rspo3
treatment
18hr BrdU
pulse
Flow cytometry
analysis
Day 1, 3
Day 5
Day 6
K
Count
119
89
60
30
0
0 cycle
1 cycle
2 cycles
APC-A
L
Count
147
110
74
37
0
0 cycle
1 cycle
2 cycles
APC-A
M
% of cells BrdU+
80
60
40
20
0
Control
Rspo3
0
1
2
0
1
2

Figure 6. Conservation of Identified Compartment-Specific Markers in Human Scalp Hair Follicle and Sensitivity to R-spondin Signaling

(A–E) Adult human scalp terminal hair follicle bulbs immunostained with antibodies against (A) Runx, (B) Vcan, (C) Pax1, (D) Bgn, and (E) Rspo2 (all in red). Nuclei were stained with Hoechst (gray). Scale bars, 50 μm.

(F) Secondary passage human dermal progenitor colonies grown for 14 days in the absence or presence of R-spondin2 or -3. Scale bar, 50 μm.

(G and H) Quantification of mean colony (G) number and (H) size. Mean ± SEM, n = 3 independent human samples.

(I) Adult human colony-forming dermal progenitors were cultured from scalp skin and immunostained for the R-spondin receptor, Lgr4 (red). Nuclei were stained with Hoechst (gray). Scale bar, 10 μm.

(J) Experimental outline of the BrdU pulse-chase experiment. Cells were pulsed with BrdU for 18 h before flow cytometry analysis.

(K and L) Representative flow cytometry readings of BrdU-APC-positive cells from (K) control and (L) RSPO3 treatments. The number of replication cycles were gated using positive and negative controls.

(M) Quantification of the percentage of cells in each cycle categorization determined from K and L. n = 3 independent culture samples for each group. Data are mean ± SD.

Our results also serve to extend recent work showing that intradermal injection of recombinant Rspo2 following depilation was sufficient to extend the length of anagen hair growth in mice (Smith et al., 2016). We found that exogenous R-spondins 2/3 were sufficient to induce precocious anagen in competent (telogen) HFs, likely when adequate levels of endogenous Wnts are present. We also show that a loss of DP-specific *Rspo3* caused a delay in HF regeneration during the second anagen. Although this effect was relatively modest, it is possible that other R-spondin family members (in particular *Rspo2*) may compensate for the loss of *Rspo3* (Neufeld et al., 2012). Indeed, our cell culture work suggests that RSPO2/3 may have redundant effects *in vitro*. Moreover, tamoxifen inducible Cre-recombination via the Prominin1 promoter did not initiate recombination in all DP cells (52.5 ± 9.6% of HFs exhibited tdTomato expression in DP following tamoxifen application), which may limit the phenotype following *Rspo3* deletion. Nevertheless, together, our data show that the DP is a rich source of R-spondins that stimulate proliferation of both HF epithelial progenitors and mesenchymal hfDSCs. Hence, R-spondins may serve to synchronously activate both progenitor pools to enable coordinated growth of the HF. Given that exposure to R-spondins also caused a robust increase in proliferation/self-renewal of isolated sphere-forming adult human dermal progenitors (a surrogate for hfDSCs), this may be an important regulator of cutaneous stem cells in human skin, although further work is needed.

An important finding from our compartment-specific transcriptomic profiles was the identification of several novel extracellular proteins in the DC/hfDSC population, including CD200 and ITGα5, -8, and -11. Besides indicating potential novel signaling pathways that modulate DC/CTS function, this also provides new accessible markers to enable prospective isolation of DC/CTS cells for further studies. Notably, ITGα5 also reliably marked the bulk of the anagen HF mesenchyme and prospective isolation enabled marked enrichment of human colony-forming dermal progenitors thus providing a useful tool for isolation of HF mesenchymal cells for future commercial or therapeutic applications looking into treatment of skin diseases such as chronic wound healing and skin cancers.

More generally, this work reinforces the role of R-spondins as important modulators of stem cell function and tissue regeneration in a variety of organs (Schuijers and Clevers, 2012). Our data confirm that the molecular machinery for R-spondin signaling is present in colony-forming dermal progenitors isolated from adult human scalp, which express the R-spondin receptor LGR4. Further support for this comes from Yi et al. who showed that LGR4 is present in the adult human HF epithelia and mesenchyme (Yi et al., 2013). Our results confirm that addition of R-spondin to isolated human scalp-derived dermal progenitors causes a marked increase in cell division and colony formation, closely resembling our results from rodent hfDSCs. Our cell culture work suggests that RSPO2/3 promote proliferation through the canonical Wnt pathway. Specification of hfDSCs might be further regulated by other regulators of Wnt signaling found in the HF mesenchymal signatures, such as SFRP1/2/4, secreted Wnt regulators that were abundant in the DP. Thus, Wnt signaling, in part through R-spondin potentiation, may be important for the expansion of mesenchymal progenitors from human hair follicles *ex vivo*, while maintaining their inductive capacity for future therapeutic efforts toward restoration of hair follicle growth.

Our transcriptomic characterization of the adult DP provides new insight into the signals that enable coordinated activation of multiple progenitor pools to enable the organized tissue regeneration. Although

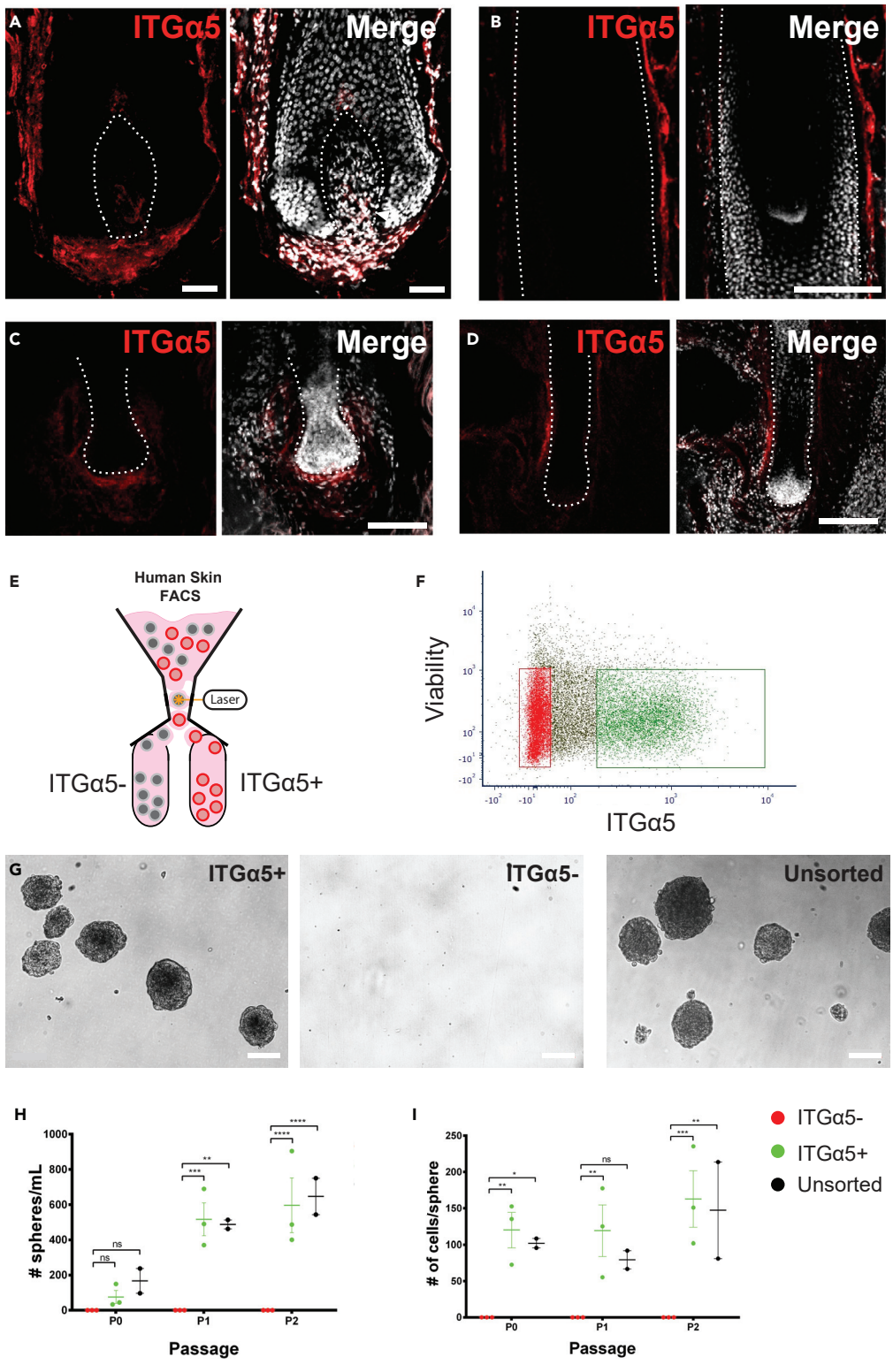

Figure 7. Itgα5^{+} Dermal Cells from Human Scalp Are Enriched for Human Dermal Progenitors

(A–D) Adult human scalp hair follicle immunostained for Itgα5 (red) and Hoechst (gray). (A) Representative image zoomed into the hair follicle bulb. Scale bar, 50 μm. (B) Representative image zoomed into the upper sheath and (C, D) low-magnification images showing the follicle and the interfollicular dermis. Scale bars, 100 μm.

Figure 7. *Continued*

(E) Experimental diagram of FACS for Itgα5^{-} and Itgα5^{+} cells from human skin.

(F) FACS isolation of Itgα5^{-} (red) and Itgα5^{+} (green) cells from dissociated human scalp tissue.

(G) Representative images of Itgα5^{+}, Itgα5^{NEG}, or unsorted dermal cells cultured for 7 days in proliferation media (one passage).

(H and I) Quantification of the (H) number of spheres/mL and number of cells/sphere (I) from each population over multiple passages. (Data are mean ± SD; *p < 0.05, **p < 0.01, ***p < 0.001, ****p < 0.0001, ANOVA Tukey).

there is considerable overlap (54 genes in common; ~26% concordance) with previously described DP signatures from neonatal skin (Rendl et al., 2005; Sennett et al., 2015), our data impart new insights into the inductive program involved in adult regeneration as opposed to developmental morphogenesis. Previous work has examined the adult telogen DP (Greco et al., 2009), but this study is the first to describe the transcriptional changes associated with the DP at the onset of adult anagen. By comparing with isolated human DP signatures, we provide a "core" adult DP signature that appears conserved across species. Identifying "definitive DP" signature genes are of paramount importance because they may indicate essential transcriptional programs that are enabled during development and recapitulated during adult regeneration.

Although we describe unique signatures for each mesenchymal compartment, there was an intriguing similarity between DP/hfDSC signatures. Indeed, our previous work showed that hfDSCs generate new DP cells that take up residence in different regions of the DP (Rahmani et al., 2014). It may be that hfDSC progeny that reside within the most proximal regions of the DP do not fully commit to a DP fate and thus represent a temporary, intermediary state. This would be consistent with our previous finding that Lef1^{+ve} hfDSCs progeny in the DP can exit this niche during catagen and subsequently re-enter the hfDSC pool following catagen remodeling of the niche (Rahmani et al., 2014). The migration and temporary residence of some hfDSCs progeny in the DP may explain the relatedness of the DP/hfDSC signature. To further investigate this similarity, we constructed an "inductive" signature, combining genes common to DP and hfDSCs that are most differentially expressed compared with the IFD cell population. These genes may hold particular importance as they represent a subset of fibroblasts that are uniquely endowed with inductive potential.

In summary, our findings provide a comprehensive molecular characterization of the adult hfDSC lineage, including their derivatives within the adult DP. R-spondins secreted from the DP appear to synchronously activate proliferation of both hfDSCs and epithelial stem/progenitors within the regenerating HF, highlighting both the source of R-spondin within the adult HF and clarifying its specific function. This work provides unique insight into the transcriptional identities of two functionally distinct compartments within the adult HF, thereby highlighting the functional diversity within tissue fibroblasts and their important contributions to tissue regeneration.

Limitations of the Study

The partial phenotype observed in our Rspo3 KO experiments may be due to redundancy by other Rspo family members within the hair follicle mesenchyme.

Validation of candidate genes is limited to gene expression owing to a lack of verified, reliable antibodies.

Although Prom1 is highly enriched in DP, its expression is not universally expressed by all DP cells and its expression varies throughout the HF cycle. As such, genetic deletion of Rspo3 using a Prom1CreERT2 driver likely does not completely abolish Rspo3 in the DP. This may further explain the partial phenotype we have observed, in addition to redundancy and partial compensation by other R-spondin family members (e.g., Rspo2).

The sorting strategy used in our experiments may not capture DP and DC populations exclusively. Cell sorting will enrich for these populations, but there is a risk of contaminating cell types that is inherent with this technique and will be included in any bulk RNA-seq preparation. This limitation is not unique to our work but a general limitation of all bulk RNA-seq experiments. Unfortunately, single cell RNA-seq technologies were not yet available at the time when this work was undertaken. This limitation necessitated the various forms of candidate target validation included in this manuscript.

METHODS

All methods can be found in the accompanying Transparent Methods supplemental file.

DATA AND CODE AVAILABILITY

RNA-seq data that support the findings of this study can be accessed through the Gene Expression Omnibus (GEO) under accession code GSE109256. Complete signature genes can be found in Table S1. All other data supporting the findings of this study are available from the corresponding author upon request.

SUPPLEMENTAL INFORMATION

Supplemental Information can be found online at https://doi.org/10.1016/j.isci.2020.101019.

ACKNOWLEDGMENTS

Sincere appreciation to Scott Magness, Larysa Pevny, and J.C. for *αSMA:dsRed*, *Sox2:GFP*, and *Rspo3^{flox}* transgenic mice, respectively, as well as to the Qingyun Liu lab for the LGR4 antibody. This work was gratefully supported by Canadian Institutes of Health Research (MOP-106646 and PJT-156444; both to J.B.) and the Calgary Firefighters Burn Treatment Society.

AUTHOR CONTRIBUTIONS

Conceptualization, A.H. and J.B.; Methodology, A.H., J.B, W.S.; Software, A.H, M.W., W.S.; Validation, A.H., E.L., H.S., N.S., S.S., W.A, W.R., W.S.; Formal Analysis, A.H., W.A., W.S.; Investigation, A.H., W.S., S.S., W.A.; Resources, I.D., N.A., J.C., J.Y., S.A., W.R.; Writing – Original Draft, A.H. and J.B.; Writing – Review & Editing, A.H., J.B, W.S; Funding Acquisition and Supervision, J.B.

DECLARATION OF INTERESTS

The authors declare no competing interests.

Received: July 30, 2019
Revised: October 18, 2019
Accepted: March 24, 2020
Published: April 24, 2020

REFERENCES

Abo, A., and Clevers, H. (2012). Modulating WNT receptor turnover for tissue repair. Nat. Biotechnol. *30*, 835–836.

Barker, N., Huch, M., Kujala, P., van de Wetering, M., Snippert, H.J., van Es, J.H., Sato, T., Stange, D.E., Begthel, H., van den Born, M., et al. (2010). Lgr5(+ve) stem cells drive self-renewal in the stomach and build long-lived gastric units in vitro. Cell Stem Cell *6*, 25–36.

Barker, N., van Es, J.H., Kuipers, J., Kujala, P., van den Born, M., Cozijnsen, M., Haegebarth, A., Korving, J., Begthel, H., Peters, P.J., et al. (2007). Identification of stem cells in small intestine and colon by marker gene Lgr5. Nature *449*, 1003–1007.

Biernaskie, J., Paris, M., Morozova, O., Fagan, B.M., Marra, M., Pevny, L., and Miller, F.D. (2009). SKPs derive from hair follicle precursors and exhibit properties of adult dermal stem cells. Cell Stem Cell *5*, 610–623.

Bodo, E., Kromminga, A., Biro, T., Borbiro, I., Gaspar, E., Zmijewski, M.A., van Beek, N., Langbein, L., Slominski, A.T., and Paus, R. (2009). Human female hair follicles are a direct, nonclassical target for thyroid-stimulating hormone. J. Invest. Dermatol. *129*, 1126–1139.

Carmon, K.S., Gong, X., Lin, Q., Thomas, A., and Liu, Q. (2011). R-spondins function as ligands of the orphan receptors LGR4 and LGR5 to regulate Wnt/beta-catenin signaling. Proc. Natl. Acad. Sci. U S A *108*, 11452–11457.

Carmon, K.S., Lin, Q., Gong, X., Thomas, A., and Liu, Q. (2012). LGR5 interacts and cointernalizes with Wnt receptors to modulate Wnt/beta-catenin signaling. Mol Cell Biol *32*, 2054–2064.

Chen, B., Dodge, M.E., Tang, W., Lu, J., Ma, Z., Fan, C., Wei, S., Hao, W., Kilgore, J., WIlliams, N.S., Roth, M.G., Amatruda, J.F., Chen, C., and Lum, L. (2009). Small molecule-mediated disruption of Wnt-dependent signaling in tissue regeneration and cancer. Nat. Chem. Biol. *5*, 100–107.

Chi, W., Wu, E., and Morgan, B.A. (2015). Earlier-born secondary hair follicles exhibit phenotypic plasticity. Exp. Dermatol. *24*, 265–268.

Clavel, C., Grisanti, L., Zemla, R., Rezza, A., Barros, R., Sennett, R., Mazloom, A.R., Chung, C.Y., Cai, X., Cai, C.L., et al. (2012). Sox2 in the dermal papilla niche controls hair growth by finetuning BMP signaling in differentiating hair shaft progenitors. Dev. Cell *23*, 981–994.

de Lau, W., Peng, W.C., Gros, P., and Clevers, H. (2014). The R-spondin/Lgr5/Rnf43 module: regulator of Wnt signal strength. Genes Dev. *28*, 305–316.

Driskell, R.R., Giangreco, A., Jensen, K.B., Mulder, K.W., and Watt, F.M. (2009). Sox2-positive dermal papilla cells specify hair follicle type in mammalian epidermis. Development *136*, 28152823.

Greco, V., Chen, T., Rendl, M., Schober, M., Pasolli, H.A., Stokes, N., Dela Cruz-Racelis, J., and Fuchs, E. (2009). A two-step mechanism for stem cell activation during hair regeneration. Cell Stem Cell *4*, 155–169.

Higgins, C.A., Chen, J.C., Cerise, J.E., Jahoda, C.A., and Christiano, A.M. (2013). Microenvironmental reprogramming by three-dimensional culture enables dermal papilla cells to induce de novo human hair-follicle growth. Proc. Natl. Acad. Sci. U S A *110*, 19679–19688.

Hsu, Y.C., Li, L., and Fuchs, E. (2014). Transit-amplifying cells orchestrate stem cell activity and tissue regeneration. Cell *157*, 935–949.

Hsu, Y.C., Pasolli, H.A., and Fuchs, E. (2011). Dynamics between stem cells, niche, and progeny in the hair follicle. Cell *144*, 92–105.

Jahoda, C.A., Horne, K.A., and Oliver, R.F. (1984). Induction of hair growth by implantation of cultured dermal papilla cells. Nature (311), 560–562.

Jaks, V., Barker, N., Kasper, M., van Es, J.H., Snippert, H.J., Clevers, H., and Toftgard, R. (2008). Lgr5 marks cycling, yet long-lived, hair follicle stem cells. Nat. Genet. *40*, 1291–1299.

Joost, S., Zeisel, A., Jacob, T., Sun, X., La Manno, G., Lonnerberg, P., Linnarsson, S., and Kasper, M. (2016). Single-cell transcriptomics reveals that differentiation and spatial signatures shape epidermal and hair follicle heterogeneity. Cell Syst. *3*, 221–237 e229.

Kobielak, K., Pasolli, H.A., Alonso, L., Polak, L., and Fuchs, E. (2003). Defining BMP functions in the hair follicle by conditional ablation of BMP receptor IA. J. Cell Biol. *163*, 609–623.

McElwee, K.J., Kissling, S., Wenzel, E., Huth, A., and Hoffmann, R. (2003). Cultured peribulbar dermal sheath cells can induce hair follicle development and contribute to the dermal sheath and dermal papilla. J. Invest. Dermatol. *121*, 1267–1275.

Neufeld, S., Rosin, J.M., Ambasta, A., Hui, K., Shaneman, V., Crowder, R., Vickerman, L., and Cobb, J. (2012). A conditional allele of Rspo3 reveals redundant function of R-spondins during mouse limb development. Genesis *50*, 741–749.

Niida, A., Hiroko, T., Kasai, M., Furukawa, Y., Nakamura, Y., Suzuki, Y., Sugano, S., and Akiyama, T. (2004). DKK1, a negative regulator of Wnt signaling, is a target of the beta-catenin/TCF pathway. Oncogene *23*, 8520–8526.

Ohyama, M., Kobayashi, T., Sasaki, T., Shimizu, A., and Amagai, M. (2012). Restoration of the intrinsic properties of human dermal papilla in vitro. J. Cell Sci. *125*, 4114–4125.

Ohyama, M., Terunuma, A., Tock, C.L., Radonovich, M.F., Pise-Masison, C.A., Hopping, S.B., Brady, J.N., Udey, M.C., and Vogel, J.C. (2006). Characterization and isolation of stem cell enriched human hair follicle bulge cells. J. Clin. Invest. *116*, 249–260.

Oshimori, N., and Fuchs, E. (2012). Paracrine TGF-beta signaling counterbalances BMPmediated repression in hair follicle stem cell activation. Cell Stem Cell *10*, 63–75.

Rahmani, W., Abbasi, S., Hagner, A., Raharjo, E., Kumar, R., Hotta, A., Magness, S., Metzger, D., and Biernaskie, J. (2014). Hair follicle dermal stem cells regenerate the dermal sheath, repopulate the dermal papilla, and modulate hair type. Dev. Cell *31*, 543–558.

Rendl, M., Lewis, L., and Fuchs, E. (2005). Molecular dissection of mesenchymal-epithelial interactions in the hair follicle. PLoS Biol. *3*, e331.

Rendl, M., Polak, L., and Fuchs, E. (2008). BMP signaling in dermal papilla cells is required for their hair follicle-inductive properties. Genes Dev. *22*, 543–557.

Rezza, A., Wang, Z., Sennett, R., Qiao, W., Wang, D., Heitman, N., Mok, K.W., Clavel, C., Yi, R., Zandstra, P., et al. (2016). Signaling networks among stem cell precursors, transit-amplifying progenitors, and their niche in developing hair follicles. Cell Rep. *14*, 3001–3018.

Rompolas, P., Deschene, E.R., Zito, G., Gonzalez, D.G., Saotome, I., Haberman, A.M., and Greco, V. (2012). Live imaging of stem cell and progeny behaviour in physiological hair-follicle regeneration. Nature *487*, 496–499.

Ruffner, H., Sprunger, J., Charlat, O., Leighton-Davies, J., Grosshans, B., Salathe, A., Zietzling, S., Beck, V., Therier, M., Isken, A., et al. (2012). R-Spondin potentiates Wnt/beta-catenin signaling through orphan receptors LGR4 and LGR5. PLoS One *7*, e40976.

Sato, T., Vries, R.G., Snippert, H.J., van de Wetering, M., Barker, N., Stange, D.E., van Es, J.H., Abo, A., Kujala, P., Peters, P.J., et al. (2009). Single Lgr5 stem cells build crypt-villus structures in vitro without a mesenchymal niche. Nature *459*, 262–265.

Schuijers, J., and Clevers, H. (2012). Adult mammalian stem cells: the role of Wnt, Lgr5 and Rspondins. EMBO J. *31*, 2685–2696.

Sennett, R., Wang, Z., Rezza, A., Grisanti, L., Roitershtein, N., Sicchio, C., Mok, K.W., Heitman, N.J., Clavel, C., Ma'ayan, A., et al. (2015). An integrated transcriptome atlas of embryonic hair follicle progenitors, their niche, and the developing skin. Dev. Cell *34*, 577–591.

Smith, A.A., Li, J., Liu, B., Hunter, D., Pyles, M., Gillette, M., Dhamdhere, G.R., Abo, A., Oro, A., and Helms, J.A. (2016). Activating hair follicle stem cells via R-spondin2 to stimulate hair growth. J. Invest. Dermatol. *136*, 1549–1558.

Taylor, G., Lehrer, M.S., Jensen, P.J., Sun, T.T., and Lavker, R.M. (2000). Involvement of follicular stem cells in forming not only the follicle but also the epidermis. Cell *102*, 451–461.

Tumbar, T., Guasch, G., Greco, V., Blanpain, C., Lowry, W.E., Rendl, M., and Fuchs, E. (2004). Defining the epithelial stem cell niche in skin. Science *303*, 359–363.

van der Flier, L.G., and Clevers, H. (2009). Stem cells, self-renewal, and differentiation in the intestinal epithelium. Annu. Rev. Physiol. *71*, 241–260.

Wang, L.C., Liu, Z.Y., Gambardella, L., Delacour, A., Shapiro, R., Yang, J., Sizing, I., Rayhorn, P., Garber, E.A., Benjamin, C.D., et al. (2000). Regular articles: conditional disruption of hedgehog signaling pathway defines its critical role in hair development and regeneration. J. Invest. Dermatol. *114*, 901–908.

Yi, J., Xiong, W., Gong, X., Bellister, S., Ellis, L.M., and Liu, Q. (2013). Analysis of LGR4 receptor distribution in human and mouse tissues. PLoS One *8*, e78144.

Zhou, L., Xu, M., Yang, Y., Yang, K., Wickett, R.R., Andl, T., Millar, S.E., and Zhang, Y. (2016). Activation of beta-catenin signaling in CD133-positive dermal papilla cells drives postnatal hair growth. PLoS One *11*, e0160425.

iScience, Volume *23*

Supplemental Information

Transcriptional Profiling of the Adult Hair Follicle Mesenchyme Reveals R-spondin as a Novel Regulator of Dermal Progenitor Function

Andrew Hagner, Wisoo Shin, Sarthak Sinha, Whitney Alpaugh, Matthew Workentine, Sepideh Abbasi, Waleed Rahmani, Natacha Agabalyan, Nilesh Sharma, Holly Sparks, Jessica Yoon, Elodie Labit, John Cobb, Ina Dobrinski, and Jeff Biernaskie

Supplementary Figure Legends

Supplementary Figure S1: Compartment-specific staining within the adult hair follicle mesenchyme. Related to Figure 1.

(A-E) Immunostaining in the adult hair follicle for cell surface markers of dermal sheath and dermal papilla (A-B) Cd200, (C) Itgα5, (D) Itgα8 and (E) Itgα9, using fate-mapped *α*SMACreER^{T2}:ROSA^{eYFP} mice to mark mesenchymal cells for colocalization. Markers are stained in red, YFP is in green and Hoechst is in grey. Scale bar = 50 um.

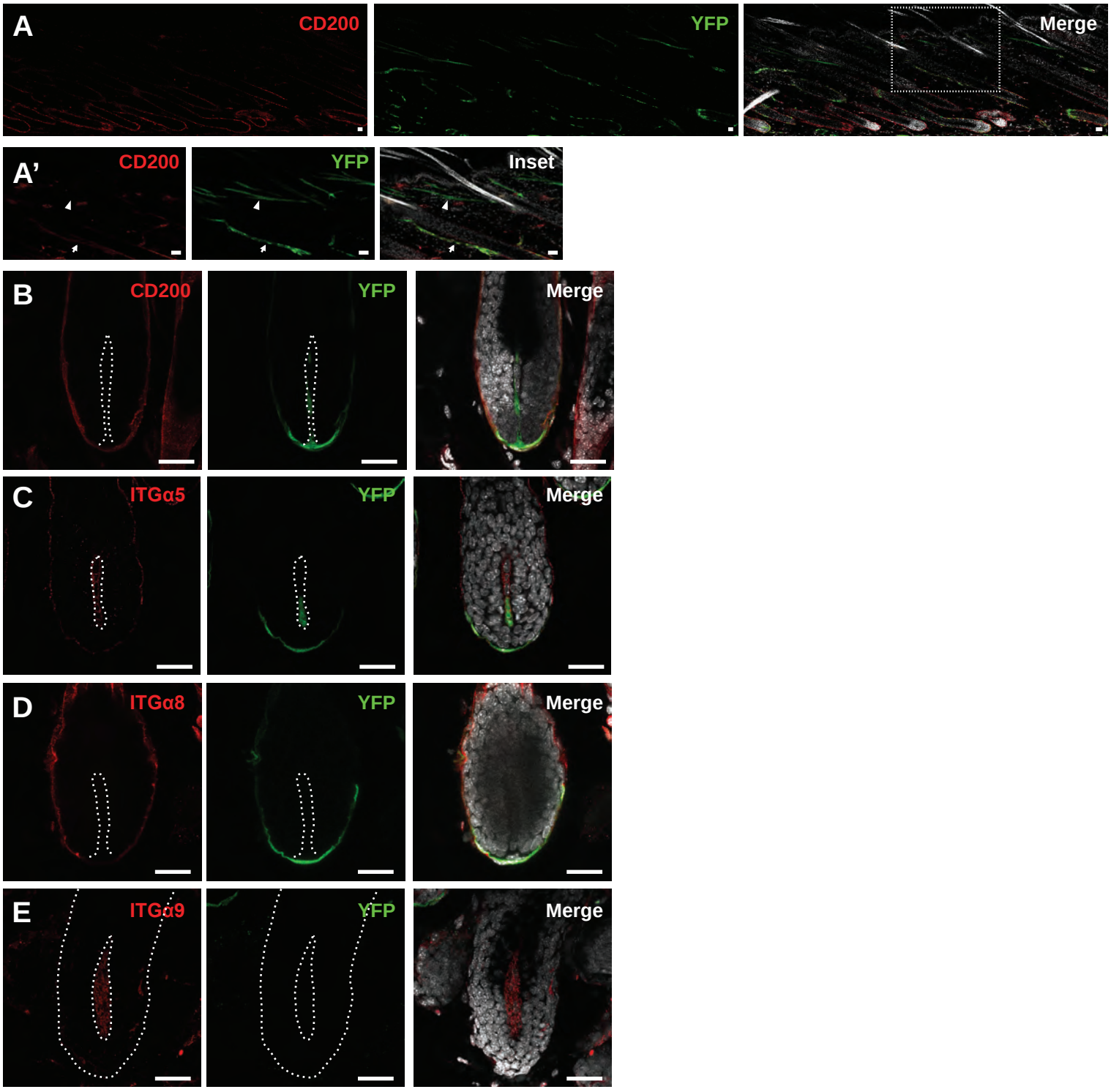
A
CD200
YFP
Merge
A'
CD200
YFP
Inset
B
CD200
YFP
Merge
C
ITGα5
YFP
Merge
D
ITGα8
YFP
Merge
E
ITGα9
YFP
Merge

Supplementary Figure S2: RNA-Seq analysis identifies hair follicle mesenchymal inductive signature. Related to Figure 2.

(A) Table of “inductive” signature genes, comprising genes (up-regulated) differentially expressed and common to DC and DP cells, as compared to IFD. Genes were excluded on a basis of q-value <0.05 and a log2-fold change >5. FPKM values for each gene and each cell population are included.

(B) Gene ontology analysis of biological processes for the “inductive” signature in (A), but expanded to include genes that are >10-fold differentially expressed, rather than based on a log2-fold change >5. A table of this extended inductive signature can be found in Supplementary Table S1.

(C-D) Venn diagram comparing the DP signature (Supplementary Table S1) and the “Core DP” signature published by Sennett et al., *Dev. Cell*, 2015. This comparison highlights the similarities and differences between adult and neonate dermal papilla signature genes. A list of the common genes can be found in (D). (E-F) Venn diagram comparing our adult mouse DP signature (Supplementary Table S1) and the human DP signatures published by Ohyama et al., *J. Cell Sci.*, 2012, and Higgins et al., *Proc. Natl. Acad. Sci.* This comparison highlights the similarities and differences between adult mouse dermal papilla and adult human dermal papilla signature genes. A list of the common genes can be found in (F).

A

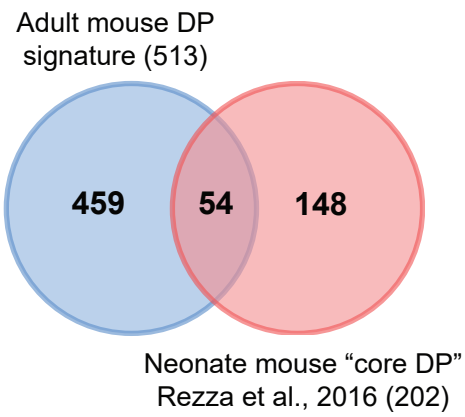

B

DP Signature/DP Core		
Chodl	Hhip	Rspo2
Clmn	Igfbp5	Rspo3
Cntn1	Itga9	Rspo4
Col23A1	Kcnn3	Scube3
Crabp1	Ldb2	Serpine2
Crabp2	Lrrtm3	Sfmbt2
Crispld1	Ltbp1	Sfrp1
Dcc	Maob	Shisa9
Dio2	Mc2R	Slc16A2
Dnali1	Ncoa7	Slc5A7
Edn3	Ndnf	Snap91
Fgf10	Nrg2	Sod3
Fgf7	Pappa	Spock3
Gdf10	Pappa2	Steap2
Gldn	Pcdh11X	Thrb
Gpr165	Piezo2	Thsd7A
Greb1L	Ptprz1	Trpm3
Grin3A	Rab39B	Zcchc18

C

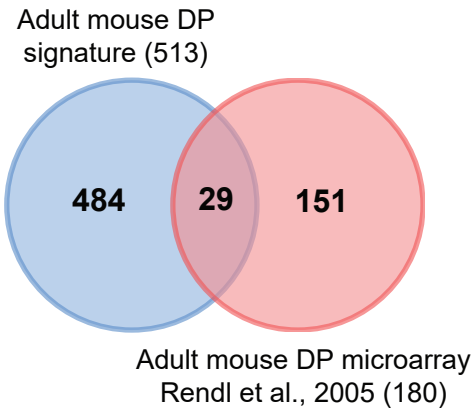

D

DP signature		
Cebpa	Gdf10	Prlr
Chodl	Gpx3	Ptprz1
Cntn1	Hhip	S100b
Crabp1	Hs3st1	Sfrp2
Crabp2	Inhba	Slc16a2
Dio2	Itga9	Snap91
Edn3	Ltbp1	Sostdc1
Fgf10	Nkd2	Sox2
Fgf7	Pappa	Zic3
Fst	Prdm1	

E

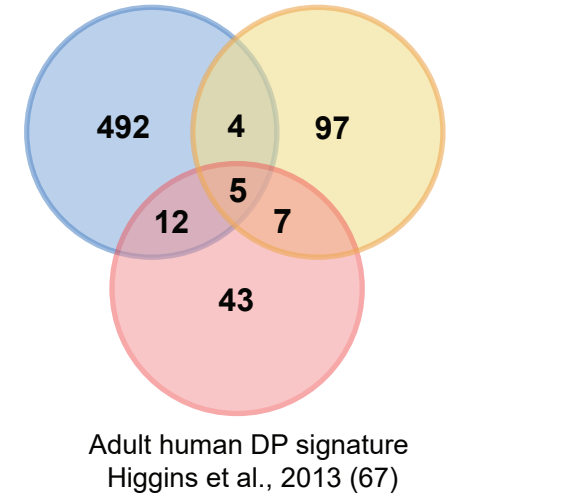

F

mDP sig vs. Higgins huDP
Chodl
Crabp1
Gpx3
Hhip
Itm2A
Pappa2
Pi15
Rspo2
S100B
Sfrp1
Sfrp2
Sostdc1

mDP sig vs. Ohyama huDP
Clca2
Pik3R1
Ptgs2
Tmem100

All combined
A2M
Dio2
Edn3
Gpm6B
Sparcl1

mDP sig vs. Higgins huDP
Aqp1
Lamc3
Lpl
Mgp
Sfn
Spon1
Wif1

Supplementary Figure S3: Receptor-ligand interactions mediating cellular communication in quiescent and regenerating hair follicles. Related to Figure 2.

Three tables list potential direct receptor-ligand protein interactions between adult dermal papilla signature genes and anagen epithelial, telogen epithelial, and anagen mesenchymal cell populations (hfDSCs: hair follicle dermal stem cells; ORS: outer root sheath; TACs: transit-amplifying cells (epithelial)).

Epithelial (anagen)

Dermal papilla : Bulge/ORS

Ptprz1 — Tnf

Il1r2 — Il1a

Rspo1-4 — Lgr5

Dermal papilla : Matrix/TACs

Sfrp4 — Fbln1

Sfrp1 — Wnt8a

Hhip — Shh

Aloxe3 — Tgm1

Dermal papilla : Melanocytes

Ly6d — Pkib

Edn3 — Ednrb

Nrg2 — Erbb4

Epithelial (telogen)

Dermal papilla : Bulge

Gpc6 — Fgf1

Dermal papilla : Hair germ

Sfrp1 — Thbs1

Sfrp2 — Thbs1

Fst — Adam8

Mesenchymal (anagen)

Dermal papilla : Dermal Cup

Dcc — Ntn1

Lypd3 — Endod1

Edn3 — Ednra

Edn3 — Ednrb

Receptor
Ligand
Other

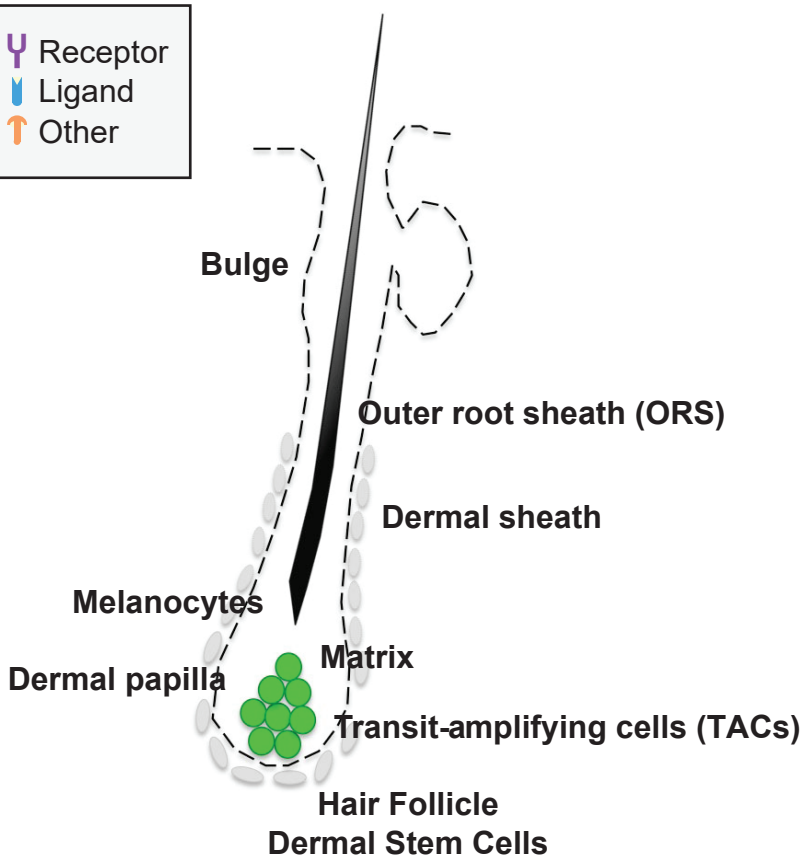

Supplementary Figure S4: RSPO2 and RSPO3 show redundant effects and promotes proliferation through the canonical Wnt pathway in vitro. Related to Figure 4 and 5.

(A) Experimental outline of the isolation of TdTomato^{+} cells from αSMACreER$^{T2:}$Rosa^{TdTomat}o mice. FACS isolated cells plated at 50,000 cells/mL and were grown in proliferation media with the treatment of drugs at day 1, 3 and 6. The cultures were analyzed for spherical colonies and total cell number at day 9.

(B) Representative images of isolated cells grown in no treatment, RSPO2, RSPO3 and both Rspo2/3. Scale bars = 200µm.

(C-D) Quantification of (C) spherical colony number and (D) total number of cells in B. n = 3 technical replicates from cells isolated from 3 biological replicate mice. *p<0.05 and ***p<0.001, ANOVA Tukey.

(E) Representative images of isolated cells grown in no treatment, DKK1, RSPO3 and RSPO3 + DKK1. Scale bars = 200µm.

(F-G) Quantification of (F) spherical colony number and (G) total number of cells in E. n = 6 technical replicates from cells isolated from 6 biological replicate mice. *p<0.05, ANOVA Tukey.

(H) Representative images of isolated cells grown in no treatment, low dose IWR cocktail called 2i (combination of 5µM IWP2 and 10µM IWR1-endo), RSPO3 and RSPO3 + 2i. Scale bars = 200µm.

(I) Total spherical colony number in H. n = 3 technical replicates from cells isolated from 3 biological replicate mice. *p<0.05, ANOVA Tukey.

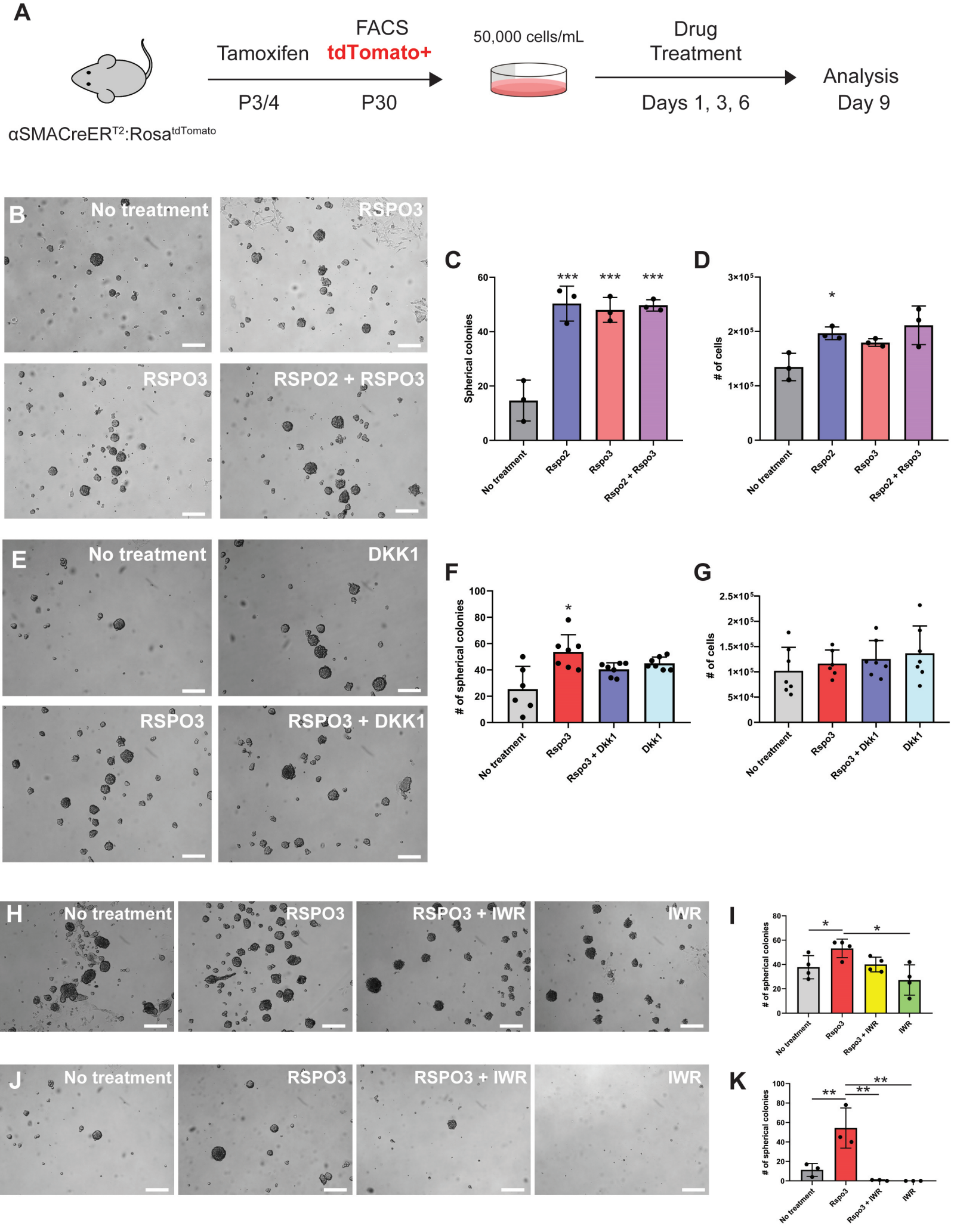
A
αSMACreER^{T2}:Rosa^{tdTomato}
Tamoxifen
P3/4
FACS
tdTomato+
P30
50,000 cells/mL
Drug
Treatment
Days 1, 3, 6
Analysis
Day 9
B
No treatment
RSPO3
RSPO3
RSPO2 + RSPO3
C
Spherical colonies
No treatment
Rspo2
Rspo3
Rspo2 + Rspo3
D
# of cells
E
No treatment
DKK1
RSPO3
RSPO3 + DKK1
F
# of spherical colonies
No treatment
Rspo3
Rspo3 + Dkk1
Dkk1
G
# of cells
H
No treatment
RSPO3
RSPO3 + IWR
IWR
I
# of spherical colonies
No treatment
Rspo3
Rspo3 + IWR
IWR
J
No treatment
RSPO3
RSPO3 + IWR
IWR
K
# of spherical colonies
No treatment
Rspo3
Rspo3 + IWR
IWR

Supplementary Figure S5: Deletion of R-spondin 3 in DS cells does not affect hair follicle regeneration. Related to Figure 5.

(A) Schematic depicting αSMACreER^{T2}:*Rspo3*$^{flox/flox}$ mice generated to specifically delete *Rspo3* from the dermal sheath (including hfDSCs).

(B) Experimental schedule and representative images showing hair regrowth in αSMACreER^{T2}:*Rspo3*$^{+/+}$ (top) or αSMACreER^{T2}:*Rspo3*$^{-/-}$ (bottom) mice. All mice were treated with tamoxifen at postnatal day 23, 24 to induce recombination, depilated at P60 (1PD) and at P90 (2PD). Hair regrowth was monitored for 15 days post-depilation (PD) (n=3).

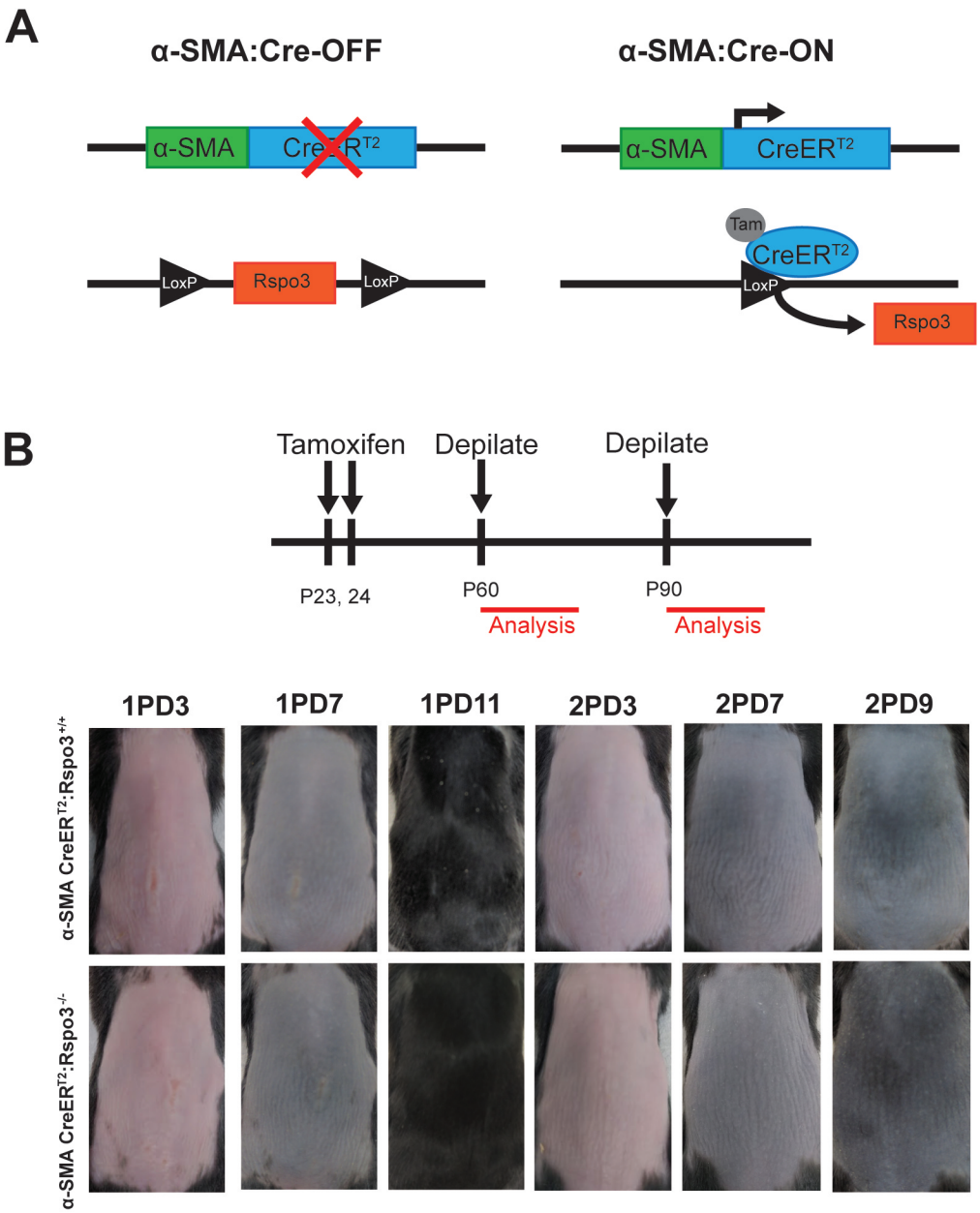
A
α-SMA:Cre-OFF
α-SMA:Cre-ON
α-SMA
CreER^{T2}
LoxP
Rspo3
LoxP
α-SMA
CreER^{T2}
Tam
CreER^{T2}
LoxP
Rspo3
B
Tamoxifen
Depilate
Depilate
P23, 24
P60
P90
Analysis
Analysis
1PD3
1PD7
1PD11
2PD3
2PD7
2PD9
α-SMA CreER^{T2}:Rspo3$^{+/+}$
α-SMA CreER^{T2}:Rspo3$^{-/-}$

Supplementary Figure S6: Treatment of human dermal progenitors with RSPO3 and CHIR elicit minute changes in proliferating and apoptotic cells. Related to Figure 6.

(A) Experimental schematic of the treatment of human dermal progenitors with RSPO3 and/or CHIR before flow cytometry analysis. n = 3 technical culture replicates from 1 biological human sample.

(B, C) Representative flow cytometry plots for (B) $Ki67^+$ and (C) $Casp3^+$ cells in human dermal progenitors. Negative and positive isotype controls were used to define positive gates.

(D) Percentage of all cells positive for Ki67 in no treatment, RSPO3 and RSPO3 + CHIR treatment groups. *p<0.05, **p<0.01, ANOVA Tukey.

(E) Percentage of all cells positive for Casp3 in no treatment, RSPO3 and RSPO3 + CHIR treatment groups. ****p<0.0001, ANOVA Tukey.

(F) Total number of cells after 7 days of culture in no treatment, RSPO3 and RSPO3 + CHIR treatment groups. *p<0.05, ANOVA Tukey.

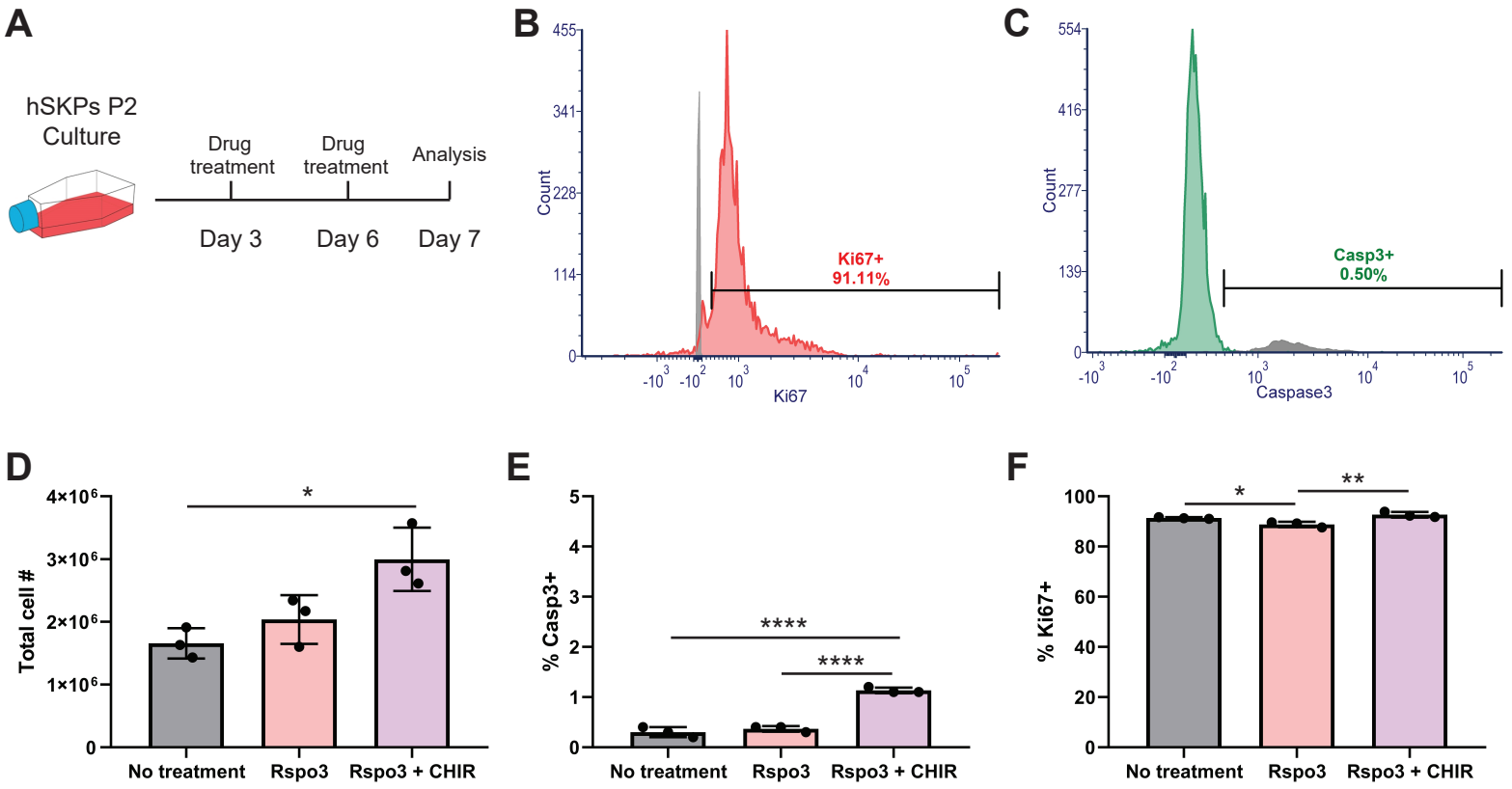
A
hSKPs P2
Culture
Drug
treatment
Drug
treatment
Analysis
Day 3
Day 6
Day 7
B
Count
Ki67+
91.11%
Ki67
C
Count
Casp3+
0.50%
Caspase3
D
Total cell #
No treatment
Rspo3
Rspo3 + CHIR
E
% Casp3+
No treatment
Rspo3
Rspo3 + CHIR
F
% Ki67+
No treatment
Rspo3
Rspo3 + CHIR

Supplementary Table S2: Antibodies. Related to Figures 1, 3, 4, 6, and 7.

Antibodies used for immunohistochemistry, immunocytochemistry and FACS, including supplier information and concentrations used.

Antibody Target	Catalogue #	Supplier	Cellular Location	Concentration
CD200/OX2	ab33734	abcam	Membrane	1:200
ITGα5	ab150361	abcam	Membrane	1:100
ITGα8	AF4076	R&D systems	Membrane	1:200
ITGα9	AF3827	R&D systems	Membrane	1:100
LGR4	(clone 5A3)	Qingyun Liu Lab	Membrane	1:50
Pax1	ab95227	abcam	Nucleus	1:100
Rspo2	ab73761	abcam	Extracellular	1:50
Runx	ab92336	abcam	Nucleus	1:200
Versican (B)	AB1033	EMD Millipore	Extracellular, organelle	1:500
αSMA	MADT381	Millipore	Cytoplasm	1:250
Krt5	PRB-160P	Covance	Cytoplasm	1:500
Ki67	4328926	Invitrogen	Nucleus	1:100
Caspase3	ab13847	Abcam	Cytoplasm	1:100
hITGα5	328009	eBioscience	Membrane	1:100

Supplementary Table S3: RNAScope Probes. Related to Figure 3.

Antibody Target	Catalogue #	Supplier
Rspo3	402011-C3	ACDBio
Spock3	545651	ACDBio
Adamts18	452251	ACDBio
Lgr4	318328	ACDBio
Lgr6	404961	ACDBio
Positive control	320881	ACDBio
Negative control	320871	ACDBio

Supplementary Table S4: qPCR Probes. Related to Figure 3.

Contains the list of genes tested by qPCR (Fig 3A-C) and the associated Taqman Assay IDs.

Gene Symbol	ThermoFisher Taqman Assay ID
Epha3	Mm00580743_m1
Fgf7	Mm00433291_m1
Fzd5	Mm00445623_s1
Hey2	Mm00469280_m1
Hic1	Mm03058120_m1
Igfbp2	Mm00492632_m1
Itga11	Hs01012939_m1

Mcam	Mm00522397_m1
Pax1	Mm00435490_m1
Pcp4	Mm00500973_m1
Pdgfrl	Mm00452798_m1
Prlr	Mm04336676_m1
Rspo3	Mm01188251_m1
Sostdc1	Mm03024258_s1
Tnnt1	Mm00449089_m1
Vcan	Mm01283062_m1

Transparent Methods

Animal husbandry and handling

All procedures received prior approval of the University of Calgary Animal Care Committee and were completed in accordance with guidelines set by the Canadian Council on Animal Care. The *αSMA:dsRed* (Magness et al., 2004) , *Sox2:GFP* (Ellis et al., 2004), *αSMACreER^{T2}:RosaYFP/ αSMACreER^{T2}:RosaTdTomato* (Rahmani et al., 2014) and *Rspo3^{flox}* (Neufeld et al., 2012) mice have been previously described. To label hfDSC progeny, all *αSMACreER^{T2}:RosaYFP/ αSMACreER^{T2}:RosaTdTomato* mice were treated with 4-hydroxytamoxifen (tamoxifen;4-OHT) at P3/4 or P23/24. *Prom1CreER^{T2}* (Zhu et al., 2009) mice were obtained from Jax (stock# 017743). Unless otherwise noted, male and female mice were used for experiments.

Cell isolation

Back skin from adult postnatal day 26 male C57Bl/6 mice was treated with dispase (StemCell Technologies) for 30 mins at 37 ^{o}C to remove epidermis. Remaining dermis was dissociated using 0.2% collagenase for 2 hours at 37 ^{o}C. Cell suspensions were diluted with cold Hank's Buffered Salt Solution (HBSS; Life Technologies), strained through 40 μm cell filters (Falcon) and centrifuged at 280 X g. Cell pellets were resuspended in FACS sorting buffer (1% bovine serum album in HBSS). DP cells were identified as αSMA:dsRed-ve Sox2:GFP+ve Integrin alpha-9+ve cells. hfDSC cells were identified as αSMA:dsRed+ve Sox2:GFP+ve cells. Interfollicular dermis (IFD) were identified as αSMA:dsRed-ve Sox2GFP-ve Integrin alpha-8-ve. FACS-isolation was performed using a FACSAria III (BD Biosciences) and analyzed using FlowJo software. All sort panels included eFluor 780 viability dye (eBioscience) to exclude dead cells and debris. Single colour and appropriate isotype controls were used for compensation and gating. Post-sort analysis showed approximately 94-98% purity. After sorting, cells were again washed in HBSS, centrifuged and the cell pellet was stored at -80 ^{o}C.

RNA isolation, sequencing, and analysis

Due to the infrequency of target cells within each mesenchymal population, cells were FACS isolated from multiple animals (6, 8, 3 and 3 animals each for DP, DC and IFD, respectively) and pooled. mRNA was isolated directly from frozen cell pellets using Dynabeads mRNA DIRECT Micro Purification Kit (Ambion). RNA sample quality and quantity were then analyzed using a 2200 Tapestation (Agilent) and a Qubit 2.0 fluorometer and sequenced using the SOLiD 5500xl system (Applied Biosystems), and were sequenced to a depth of (3.5-5) x 10^7 reads per library. Aligned sequence data was analyzed first for QC using JMP Genomics software, then using the Cufflinks software package to obtain differentially expressed signature genes for further functional analysis (Trapnell et al., 2013; Trapnell et al., 2012; Trapnell et al., 2010). Gene expression was further characterized using Panther and Ingenuity Pathway Analysis (Mi et al., 2013). GO analysis was performed on signature genes with Panther version 10.0 Release 2015-05-15, using an overrepresentation test (release 20150430, $p<0.05$) and Bonferroni correction for multiple testing against *Mus musculus* reference list, using select categories from complete annotation data sets (Mi et al., 2016).

Immunohistochemistry

Adult C57Bl/6 back skin and adult human scalp skin were fixed with 2% paraformaldehyde overnight, washed 3x in PBS and incubated in 30% sucrose overnight before being snap frozen in Clear Frozen Section Compound (VWR). Frozen tissue blocks were sectioned using a Leica 3050S cryostat at 20-50 µm onto Superfrost slides (Fisher) and stored at -80 ^{o}C. Alternatively, fresh back skin was snap frozen as above, and then fixed on slide for <10 min in 4% PFA. Frozen tissue sections were rehydrated using PBS, then blocked with 10% normal serum containing 0.3% Triton-X100 for 45 mins. Primary antibodies were incubated overnight at 4 ^{o}C, washed 3x with PBS and then incubated with Alexa Fluor secondary antibodies (Invitrogen) at 1:1,000 for 1 hour. After 1x PBS wash, sections were stained with 1 ug/mL of Hoechst 33258 for 5 minutes and washed again 3x in PBS before covering with Permafluor (Thermo Scientific) and a cover slip. Imaging was done with an Observer epifluorescence (Zeiss)

or SP8 spectral confocal microscope (Leica). A list of antibodies can be found in **Supplementary Table S2**.

In situ hybridization with RNAScope

RNAscope was performed according to manufacture instructions, using only materials provided in the RNAScope 2.0 HD Assay kit (ACDBio). In brief, frozen, fixed tissue sections were thawed from -80°C storage and allowed to dry for 30 minutes. The slides were washed with PBS for 5 minutes and antigen retrieval was performed for 5 minutes in boiling antigen retrieval solution provided in the kit (ACDBio). Slides were washed with 100% EtOH and then treated with Protease 3 (ACDBio) for 40 minutes at 40°C. After washing 2x with ddH20 (ACDBio) for 5 mins, slides were incubated in 1:50 dilutions of select probes (ACDBio) for 2 hrs in 40°C. After washing with wash buffer (ACDBio), the slides were incubated with AMP1 (ACDBio) for 30 min, AMP2 (ACDBio) for 15 min, AMP3 (ACDBio) for 30 min and AMP4 (ACDBio) for 15 min at 40°C. DAPI staining (ACDBio) was introduced for 1 min before the final wash. For tissues acquire from *αSMACreER^{T2}:RosaYFP* mice, the mice were treated with 4-OHT at P3/4 and the backskin was collected at P28. Information for all probes used in this report are found in **Supplementary Table S3**.

RT-qPCR

Total RNA was purified from FACS-sorted cell populations as above. FAM or Vic TaqMan probes (Life Technologies) were used. RNA (27.6 µg) was reverse transcribed using High Capacity cDNA synthesis kit (Applied Biosystems). cDNA samples were then amplified for 14 cycles using TaqMan PreAmp Master Mix Kit (Applied Biosystems) as per manufacturer's instructions. Preamplification uniformity was evaluated by comparing the ΔΔCT for each TaqMan probe from a non-limiting sample of unsorted dermal cells that had been amplified to the same sample that had not been amplified. Quantitative PCR was performed using TaqMan Fast Advanced Master Mix and samples were run using 7500 Fast Real Time PCR system (Applied Biosystems). Foldchange in gene expression was calculated using the ΔΔCT method with *hprt* serving as housekeeping gene. Each cell population of interest (DP and DC) was

compared to the control IFD population with expression set to 1. A list of assay reference IDs for each probe set can be found in **Supplementary Table S4**.

In vitro proliferation assays

Mouse hfDSCs were FACS-isolated from adult early anagen (p26) back skin and grown in bFGF (50 ng/mL, Peprotech), 1% B27 Supplement (Life Technologies) and 1% pen/strep (StemCell Technologies) for 10 days 37 ^{o}C, in presence or absence of recombinant mouse TGFβ2 (0.04 ng/uL, R&D Systems), RSPO2/3 (0.2 ng/uL, R&D Systems) and/or the Wnt agonist CHIR99021 (3 uM, StemCell Technologies). Control cultures received either equivalent volumes of vehicle (PBS or DMSO) respectively. Similar to above, second passage human dermal colony-forming progenitors were grown in the presence or absence of RSPO2/3 for 14 days and proliferation was assessed. Epithelial cells were isolated from mouse back skin (see Animals, cell isolation and FACS section above) and grown in mouse Keratinocyte-SFM medium (ThermoFisher) in 96-well format. Back skin from postnatal day 2 C57Bl/6 mice was treated with dispase (StemCell Technologies) to remove epidermis. Epidermis was then floated on 0.25% Trypsin and hair follicle buds were scraped using a scalpel and filtered. Epithelial buds were then dissociated to single cells using Trypsin and were plated at 2 x 10^4 cells/mL in the presence or absence of RSPO2/3 for 3 weeks. Colony number and size were then quantified for each condition. Colonies were tracked over time, and in the case of merged colonies, size was estimated based on colony edge upon merging. Images for quantification of colony size and number in multiwell plates were obtained using an Observer inverted epifluorescence microscope (Carl Zeiss) or IN Cell Analyzer (GE Healthcare Life Sciences) and measured using Zeiss Axiovision software. Unless otherwise stated, colonies were identified as having a minimum diameter of 75 μm.

In vitro drug treatment assays

aSMACreER^{T2}:RosaTdTomato mice were treated with tamoxifen at P23/24 to label all hfDSC progeny including CTS and some DP cells (Rahmani et al., 2014). The backskin was collected from mice p28-30 and dissociated into single cells as previously

described in the “Cell isolation” section. TdTomato+ cells were collected using a FACSAria II (BD Biosciences) cell sorter and cultured in proliferation media at concentrations of 50,000cells/mL as above (Figure S4A). Primary culture cells were treated with RSPO2 (0.2ng/uL, R&D Systems), RSPO3 (0.2 ng/uL, R&D Systems), DKK1 (10ng/mL, R&D Systems), and/or a combination of IWP2 (5μM or 7.5μM, Tocris Bioscience) and IWR1-endo (10μM or 15μM, Tocris Bioscience) at culture day 1, 3 and 6. Spherical colony numbers and total number of cells were quantified at day 9.

Intradermal injections of candidate recombinant proteins

Recombinant TGFβ2 (100 ng; R&D Systems), R-spondin2 and -3 (400 ng; R&D Systems), or 0.1% BSA (vehicle controls) were co-injected with 2 μL red fluorescent FluoSpheres (Life Technologies) in αSMA:CreER^{T2}:Rosa^{YFP} mice. All injections starting at mid-telogen (P55-57) and were injected for three consecutive days. Hair growth was photographed daily at the injection sites for two weeks.

Rspo3 *in vivo* conditional deletion

For deletion of *Rspo3* in adult DP cells, *Rspo3*$^{flox/flox}$ mice were crossed with a Prom1CreER^{T2} mice. Prom1CreER^{T2}:*Rspo3*$^{flox/flox}$ and Prom1CreER^{T2}:*Rspo3*$^{+/+}$ were treated with 4OHT by intraperitoneal injection (0.25 mg or 1 mg per neonatal or adult mouse, respectively) at P2-4 (n=3), P2-4,20-21 (n=1) or P20-24 (n=4). Images were taken at P25, 27 and 30 to determine the onset of hair regeneration. Quantification of HF cycle stage was completed using a previously published classification system (Müller-Röver et al., 2001). Anagen I-II were classified as “early anagen”, Anagen IIIa-IV were classified as “mid anagen” and Anagen V-VI were classified as “late anagen”. A total of 50 HFs were analyzed from each animal. To assess the specificity of *Rspo3* deficiency, αSMACreER^{T2} mice (where Cre is expressed specifically in the HF dermal sheath) were also crossed with *Rspo3*$^{flox/flox}$ mice. αSMACreER^{T2}:*Rspo3*$^{flox/flox}$ and αSMACreER^{T2}:*Rspo3*$^{+/+}$ were treated with tamoxifen at postnatal days 3 and 4 and again at P23 and P24 (n=3). Back skin was depilated at P60 and hair regeneration was tracked until P90. Back skin was depilated for the second time on P90 and tracked to determine onset of hair regeneration.

Human dermal progenitor culture

Human skin was obtained through the Southern Alberta Tissue Recovery and Transplant Program. All experiments using human skin cells received prior approval from the Conjoint Health Research Ethics Board at the University of Calgary. As a surrogate for human hfDSCs, second passage human dermal progenitors (a.k.a skin-derived precursors; 'SKPs') were isolated and grown as non-adherent colony-forming cells as previously described (González et al., 2017; Hagner and Biernaskie, 2013; Toma et al., 2005) from the discarded surgical scalp skin of three independent human patients (2 male, 1 female), ranging from 46 to 74 year of age. Briefly, hair was trimmed, exterior skin surface was washed with 70% ethanol and underlying fat debrided. Skin floated on dispase (5 mg/mL, STEMCELL Technologies) for 4 hrs at 37°C. The epidermis was then manually removed with fine forceps and dermis was minced using scalpels and incubated in collagenase IV (2 mg/mL, Worthington) in a water bath at 37°C for 4 hours. Tissue was triturated hourly and supernatant was collected, filtered through a 70 μm filter and centrifuged for 6 mins at 200 rcf. After 4 hrs, the total cell suspension was centrifuged and then resuspended in proliferation media (PM), containing basic fibroblast growth factor (bFGF, 40 ng/mL, BD Biosciences), platelet-derived growth factor-BB (PDGF-BB, 25 ng/mL, BD Biosciences), B27 Supplement (2%, Invitrogen), penicillin/streptomycin (1%, Invitrogen) and fungizone (0.4%, Invitrogen) in DMEM low glucose/F12 (3:1, Invitrogen). Cells were plated at 24,000 cells/cm^2 and fed every 3-4 days. For colony formation assays, primary colonies were dissociated using collagenase IV (2 mg/mL, Worthington) to single cells and resuspended at a density of 10,000 cells per mL in proliferation media. Cells (n=4 replicates per condition) were fed with 80 ng/well fresh media every 4 days. After 14 days, the cells were fixed using 2% paraformaldehyde. Wells were imaged and colonies counted and measured using an Observer inverted epifluorescence microscope (Zeiss). Human dermal progenitors were then stained for LGR4 (Rat, clone 5A3; generously provided by the Qingyun Liu Lab, University of Texas).

Flow cytometry analysis of human dermal progenitors

Human dermal progenitors were isolated and cultured as previously described in the “Human dermal progenitor culture” section and passaged twice before experimentation. Second passage cells were treated with RSPO3 (0.2 ng/uL, R&D Systems), or a combination of RSPO3 (0.2 ng/uL, R&D Systems) and CHIR99021 (3 uM, StemCell Technologies) at days 1, 3 and 6 (Figure S6A). At day 7, all media including cells were transferred into a 15mL canonical tube and spun down at 200 rcf for 6 min before removing the supernatant. The cell pellet was resuspended in 1mL of collagenase IV (2 mg/mL, Worthington), incubated in a 37°C water bath at for 10 minutes and triturated every 5 minutes to dissociate into single cells. The cell solutions were topped up to 10mL with PBS, filtered through a 70µm filter and spun down at 200 rcf for 6 minutes. Supernatant was removed and the cell pellet was resuspended in 1mL of 4% PFA in PBS to fix the cells for 10 minutes on ice. At this point, a 10uL sample was taken from each sample to count the total number of cells. The fixed cell solution was washed and spun down at 200rcf for 6 minutes. The supernatant was removed and then cell pellet was resuspended in 0.5% Triton-x in PBS for 10 minutes at room temperature. After wash and removal of supernatant, the cells were resuspended in 1uL/million cells of primary antibodies in 1% BSA in HBSS () and incubated at room temperature for 30 minutes. The cells were washed, spun and the supernatant was removed. Resuspended in 0.1uL/million cells of appropriate secondary antibodies (Invitrogen) for 15 minutes before washing. The stained cells were transferred on ice for flow cytometry analysis. Flow cytometry was performed using FACSAria III (BD Biosciences) and analyzed using FlowJo software. Single colour and appropriate isotype controls were used for compensation and gating.

BrdU pulse chase

Human dermal progenitor cells were isolated and cultured to second passage. The second passage cells were grown in proliferation media, as mentioned previously and treated with RSPO3 (0.2 ng/uL, R&D Systems) at days 1, 3 (Figure 6J). At days 5, the cells were treated with BrdU (1mM) from the BD Pharmingene BrdU Flow Kit

(BDBioscience) and chased for 18 hours. After 18 hours of BrdU chase, the cells and media were collected and stained for BrdU as per manufacture protocol (BDBioscience). 7-AAD staining was omitted from the protocol. Flow cytometry was performed using a FACSAria III (BD Biosciences) and analyzed using FlowJo software. Negative and positive controls were used for compensation and gating.

Antibodies

A full list of primary antibodies for immunohistochemistry and FACS can be found in **Supplementary Table S2**. Secondary antibodies Alexa fluor 488, 555 and 647 (Invitrogen) were used to detect primary antibodies. For FACS, Alexa 647 (Life Technologies) was used with primary antibodies. All sort panels included eFluor 780 viability dye (eBioscience).

Statistics and reproducibility

For the main RNA-Seq analysis, Cufflinks software was used to determine differential expression, while the analysis of adult telogen hair germ, bulge and DP used limma software. All other statistical calculations were performed using Graphpad Prism 5. Variance for all data is expressed as ± standard error of the mean. Statistical tests used to determine significance for each experiment is stated in the corresponding figure legend. A p-value <0.05 was considered significant. The investigators were not blinded during experiments. All experiments used at least $n = 3$ biological replicates as described in each figure legend. No statistical method was used to predetermine sample size but was based on previous work. All experiments presented were reproducible and no animals were excluded from analyses.

References

Ellis, P., Fagan, B.M., Magness, S.T., Hutton, S., Taranova, O., Hayashi, S., McMahon, A., Rao, M., and Pevny, L. (2004). SOX2, a persistent marker for multipotential neural stem cells derived from embryonic stem cells, the embryo or the adult. Dev Neurosci *26*, 148-165.

González, R., Moffatt, G., Hagner, A., Sinha, S., Shin, W., Rahmani, W., Chojnacki, A., and Biernaskie, J. (2017). Platelet-derived growth factor signaling modulates adult hair follicle dermal stem cell maintenance and self-renewal. npj Regenerative Medicine *2*, 11.

Hagner, A., and Biernaskie, J. (2013). Isolation and differentiation of hair follicle-derived dermal precursors. Methods Mol Biol *989*, 247-263.

Higgins, C.A., Chen, J.C., Cerise, J.E., Jahoda, C.A., and Christiano, A.M. (2013). Microenvironmental reprogramming by three-dimensional culture enables dermal papilla cells to induce de novo human hair-follicle growth. Proc Natl Acad Sci U S A *110*, 19679-19688. Hsu, Y.C., Li, L., and Fuchs, E. (2014). Transit-amplifying cells orchestrate stem cell activity and tissue regeneration. Cell 157, 935-949.

Magness, S.T., Bataller, R., Yang, L., and Brenner, D.A. (2004). A dual reporter gene transgenic mouse demonstrates heterogeneity in hepatic fibrogenic cell populations. Hepatology 40, 11511159.

Mi, H., Muruganujan, A., Casagrande, J.T., and Thomas, P.D. (2013). Large-scale gene function analysis with the PANTHER classification system. Nat Protoc *8*, 1551-1566.

Mi, H., Poudel, S., Muruganujan, A., Casagrande, J.T., and Thomas, P.D. (2016). PANTHER version 10: expanded protein families and functions, and analysis tools. Nucleic Acids Res *44*, D336-342.

Müller-Röver, S., Foitzik, K., Paus, R., Handjiski, B., van der Veen, C., Eichmüller, S., McKay, I.A., Stenn, K.S. (2001). A Comprehensive Guide for the Accurate Classification of Murine Hair Follicles in Distinct Hair Cycle Stages. J Invest Dermatol *117*, 3-15.

Neufeld, S., Rosin, J.M., Ambasta, A., Hui, K., Shaneman, V., Crowder, R., Vickerman, L., and Cobb, J. (2012). A conditional allele of Rspo3 reveals redundant function of R-spondins during mouse limb development. Genesis *50*, 741-749.

Ohyama, M., Kobayashi, T., Sasaki, T., Shimizu, A., and Amagai, M. (2012). Restoration of the intrinsic properties of human dermal papilla in vitro. J Cell Sci *125*, 4114-4125.

Rahmani, W., Abbasi, S., Hagner, A., Raharjo, E., Kumar, R., Hotta, A., Magness, S., Metzger, D., and Biernaskie, J. (2014). Hair follicle dermal stem cells regenerate the dermal sheath, repopulate the dermal papilla, and modulate hair type. Dev Cell *31*, 543-558.

Sennett, R., Wang, Z., Rezza, A., Grisanti, L., Roitershtein, N., Sicchio, C., Mok, K.W., Heitman, N.J., Clavel, C., Ma'ayan, A.*, et al.* (2015). An Integrated Transcriptome Atlas of Embryonic Hair Follicle Progenitors, Their Niche, and the Developing Skin. Dev Cell *34*, 577-591.

Toma, J.G., McKenzie, I.A., Bagli, D., and Miller, F.D. (2005). Isolation and characterization of multipotent skin-derived precursors from human skin. Stem Cells *23*, 727-737.

Trapnell, C., Hendrickson, D.G., Sauvageau, M., Goff, L., Rinn, J.L., and Pachter, L. (2013). Differential analysis of gene regulation at transcript resolution with RNA-seq. Nat Biotechnol *31*, 46-53.

Trapnell, C., Roberts, A., Goff, L., Pertea, G., Kim, D., Kelley, D.R., Pimentel, H., Salzberg, S.L., Rinn, J.L., and Pachter, L. (2012). Differential gene and transcript expression analysis of RNA-seq experiments with TopHat and Cufflinks. Nat Protoc *7*, 562-578.

Trapnell, C., Williams, B.A., Pertea, G., Mortazavi, A., Kwan, G., van Baren, M.J., Salzberg, S.L., Wold, B.J., and Pachter, L. (2010). Transcript assembly and quantification by RNA-Seq reveals unannotated transcripts and isoform switching during cell differentiation. Nat Biotechnol *28*, 511-515.

Zhu, L., Gibson, P., Currle, D.S., Tong, Y., Richardson, R.J., Bayazitov, I.T., Poppleton, H., Zakharenko, S., Ellison, D.W., and Gilbertson, R.J. (2009). Prominin 1 marks intestinal stem cells that are susceptible to neoplastic transformation. Nature *457*, 603-607.